NAVAL POSTGRADUATE SCHOOL

MONTEREY, CALIFORNIA

THESIS

UNDERSEA NAVIGATION OF A GLIDER UUV USING AN ACOUSTIC COMMUNICATIONS NETWORK

by

Sean P. Ouimet

September 2005

Thesis Advisor: Joseph A. Rice
Co-Advisor: Arlene A. Guest

Approved for public release; distribution is unlimited

THIS PAGE INTENTIONALLY LEFT BLANK

REPORT DOCUMENTATION PAGE			Form Approved OMB No. 0704-0188
Public reporting burden for this collection of information is estimated to average 1 hour per response, including the time for reviewing instruction, searching existing data sources, gathering and maintaining the data needed, and completing and reviewing the collection of information. Send comments regarding this burden estimate or any other aspect of this collection of information, including suggestions for reducing this burden, to Washington headquarters Services, Directorate for Information Operations and Reports, 1215 Jefferson Davis Highway, Suite 1204, Arlington, VA 22202-4302, and to the Office of Management and Budget, Paperwork Reduction Project (0704-0188) Washington DC 20503.			
1. AGENCY USE ONLY *(Leave blank)*	**2. REPORT DATE** September 2005	**3. REPORT TYPE AND DATES COVERED** Master's Thesis	
4. TITLE AND SUBTITLE: Undersea Navigation of a Glider UUV Using an Acoustic Communications Network			**5. FUNDING NUMBERS**
6. AUTHOR(S) ENS Sean P. Ouimet			
7. PERFORMING ORGANIZATION NAME(S) AND ADDRESS(ES) Naval Postgraduate School Monterey, CA 93943-5000			**8. PERFORMING ORGANIZATION REPORT NUMBER**
9. SPONSORING /MONITORING AGENCY NAME(S) AND ADDRESS(ES)			**10. SPONSORING/MONITORING AGENCY REPORT NUMBER**
11. SUPPLEMENTARY NOTES The views expressed in this thesis are those of the author and do not reflect the official policy or position of the Department of Defense or the U.S. Government.			
12a. DISTRIBUTION / AVAILABILITY STATEMENT Approved for public release; distribution is unlimited			**12b. DISTRIBUTION CODE** A
13. ABSTRACT (maximum 200 words) The US Navy is developing Seaweb undersea acoustic networking technology to enable distributed autonomous ocean sensors. An Unmanned Undersea Vehicle (UUV) can operate as a mobile node among the grid in the conduct of its own mission, using the fixed nodes as navigation reference points. The fixed grid provides a cellular communications infrastructure for command & control and data telemetry. In turn, the UUV can support the fixed grid by physically redistributing large quantities of data throughout the network or for breaching the sea surface and acting as a mobile gateway node, communicating via satellite to a command center ashore. Assimilating UUVs as network nodes significantly enhances undersea network capability, expanding the available concepts of operations. This thesis concerns the use of the fixed undersea network as a means to track the UUV and anticipates routine operations of mobile nodes in the context of fixed grids. This work is also a fundamental step toward advanced operations of fully mobile networks in the form of collaborative swarms.			
14. SUBJECT TERMS Seaweb, Slocum, glider UUV, acoustic communications, tracking, telesonar modem, dead reckoning, RACOM buoy, GPS			**15. NUMBER OF PAGES** 91
			16. PRICE CODE
17. SECURITY CLASSIFICATION OF REPORT Unclassified	**18. SECURITY CLASSIFICATION OF THIS PAGE** Unclassified	**19. SECURITY CLASSIFICATION OF ABSTRACT** Unclassified	**20. LIMITATION OF ABSTRACT** UL

NSN 7540-01-280-5500 Standard Form 298 (Rev. 2-89)
Prescribed by ANSI Std. 239-18

THIS PAGE INTENTIONALLY LEFT BLANK

Approved for public release; distribution is unlimited

UNDERSEA NAVIGATION OF A GLIDER UUV USING AN ACOUSTIC COMMUNICATIONS NETWORK

Sean P. Ouimet
Ensign, United States Navy
B.S., United States Naval Academy, 2004

Submitted in partial fulfillment of the
requirements for the degree of

MASTER OF SCIENCE IN ENGINEERING ACOUSTICS

from the

NAVAL POSTGRADUATE SCHOOL
September 2005

Author: Sean P. Ouimet

Approved by: Joseph A. Rice
Thesis Advisor

Arlene A. Guest
Co-Advisor

Kevin B. Smith
Chair, Engineering Acoustics Academic Committee

THIS PAGE INTENTIONALLY LEFT BLANK

ABSTRACT

The US Navy is developing Seaweb undersea acoustic networking technology to enable distributed autonomous ocean sensors. An Unmanned Undersea Vehicle (UUV) can operate as a mobile node among the grid in the conduct of its own mission, using the fixed nodes as navigation reference points. The fixed grid provides a cellular communications infrastructure for command & control and data telemetry. In turn, the UUV can support the fixed grid by physically redistributing large quantities of data throughout the network or for breaching the sea surface and acting as a mobile gateway node, communicating via satellite to a command center ashore. Assimilating UUVs as network nodes significantly enhances undersea network capability, expanding the available concepts of operation. This thesis concerns the use of the fixed undersea network as a means to track the UUV and anticipates routine operations of mobile nodes in the context of fixed grids. This work is also a fundamental step toward advanced operations of fully mobile networks in the form of collaborative swarms.

THIS PAGE INTENTIONALLY LEFT BLANK

TABLE OF CONTENTS

LIST OF FIGURES

LIST OF TABLES

THIS PAGE INTENTIONALLY LEFT BLANK

ACKNOWLEDGMENTS

There have been many people who were instrumental in my development at NPS. First, I have to thank my professors who have challenged me and taught me some important skills that I have used in this thesis. Next, my utmost thanks go to my two thesis advisors. Prof. Joe Rice was responsible for introducing me to Seaweb and helping me to pick this thesis topic. He was able to take my interest in undersea vehicles and ocean acoustics and merge them into a work that satisfies both of those areas. He was always there when I needed a helping hand and never hesitated to offer help when I needed it. For that, I sincerely thank him. Prof. Arlene Guest was responsible for teaching me nearly everything I know about the computer program MATLAB. Her patience never waned and she spent countless hours helping me refine my algorithm. I must also give her a good amount of credit for her idea of using the center-of-mass method of glider positioning that this thesis is based upon.

The gentlemen from SPAWAR Systems Center in San Diego were also incredibly helpful. Special thanks go to Bob Creber, Paul Baxley, Bill Marn, Brian Granger, Chris Mailey, Chris Fletcher, and Lonnie Hamme.

I must also thank the crew of the *Cypress Sea* Dive Vessel for use of their equipment and for their help with our experiment.

The members of the Naval Postgraduate School's AUV Group, including Doug Horner, Tony Healey, Sean Kragelund, Ben Wring and Jeff Weekley must also be acknowledged for getting me started with the ARIES AUV at school. While they couldn't participate in the July 2005 experiment, they were part of the foundation that helped to start these tests.

My family and friends were also very helpful and encouraging throughout my year at NPS. My parents and brother were always able to pick me up after a tough test or long week of school. They constantly gave me encouragement and let me know how proud they were of me. My fellow classmates and IGEP students were also highly encouraging and were always there to give me a break or to vent to when I needed it.

Special thanks goes to ENS Matthew Hahn, whose work I am improving on in this thesis. He took the time necessary to get me caught up on the methods used in his thesis and helped me to understand some important concepts.

My final thanks go to Kathryn. Without her encouragement, I probably would not have even come out to Monterey. She always made me feel confident that being across the country would only strengthen our relationship, which it definitely has. She encouraged me from the start and has pushed me to excel to the best of my abilities.

I. INTRODUCTION – SCOPE OF THESIS

A. UNDERSEA NAVIGATION CHALLENGES

In 2004, an undersea communications experiment called Seaweb 2004 tested an undersea vehicle's ability to communicate through a network of 40 acoustic modems on the seafloor. The vehicle used the Inertial Navigation System (INS) to determine its position. Water currents, however, affected the positioning by deflecting true motion away from perceived motion. While the vehicle may have thought it was moving toward the north, a current from the east could have deflected its true motion, giving it a northwesterly heading. This navigation error, and its tendency to increase with time, is referred to as fix expansion [1].

Without access to the Global Positioning System (GPS), the Unmanned Undersea Vehicle's (UUV) position became increasingly inaccurate. This uncertainty made it difficult to determine which network node was the closest and thus thwarted effective cellular communications at times. This problem is what this thesis hopes to rectify. [1]

B. IMPROVEMENTS USING UNDERWATER ACOUSTIC RANGING

Acoustic ranging between the UUV and the seafloor nodes can mitigate the problem of fix expansion. As the vehicle moves among the network, it can transmit an acoustic ping and receive echoes from adjacent nodes. The range from the vehicle to each node can be calculated based on the round-trip propagation time of the ping/echo exchange. These ranges can then be used to calculate the vehicle's position. Each of these positions is also independent of the previous position, eliminating the problem of fix expansion.

THIS PAGE INTENTIONALLY LEFT BLANK

II. SEAWEB/UUV SYSTEM COMPONENTS

A. THE SEAWEB FIXED GRID

A major component of the Seaweb network is the repeater node. Each node consists of a Benthos ATM 885 Acoustic Telemetry Modem, which is suspended roughly three meters above the seafloor and operates in the frequency range of 9 to 14 kHz. The entire apparatus (Figure 1) is anchored by a sandbag and lifted above the seafloor by a float. An acoustic release can be triggered to allow for it to rise to the surface and be recovered or serviced. Each release has a burn wire mechanism that initiates when it detects a coded signal. Each node in the grid has a different release code, allowing for the controlled recovery of only one node at a time. [1]

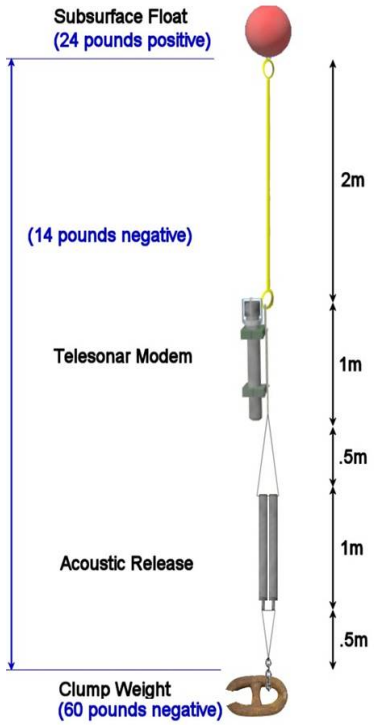

Figure 1. Seaweb Node [From 1].

1. Seaweb Undersea Communications

On land, data can be sent with good reliability and speed by radio. Radio communication is ineffective in the ocean, however, because of the large amount of attenuation that occurs in this medium. One way to send data through water, however, is

with an acoustic signal. While it is not quite as fast as a telephone line or radio link on land, undersea acoustic communications are very effective.

2. Node-to-node "Handshaking"

When one network node (node A in Figure 2) wants to pass data to another node (B), it sends a utility packet called a "request to send". This utility packet brings node B out of a low-power state (which is used to conserve energy). In response, node sends a "clear to send" utility packet back to node A. Node A then sends the data packet to node B. If any errors have occurred in the data, node B sends a "Selective Automatic Repeat Request" (SRQ) utility packet back to Node A, requesting that the erroneous data sub-packets be resent. When node A receives an SRQ, it sends the requested data to node B [2].

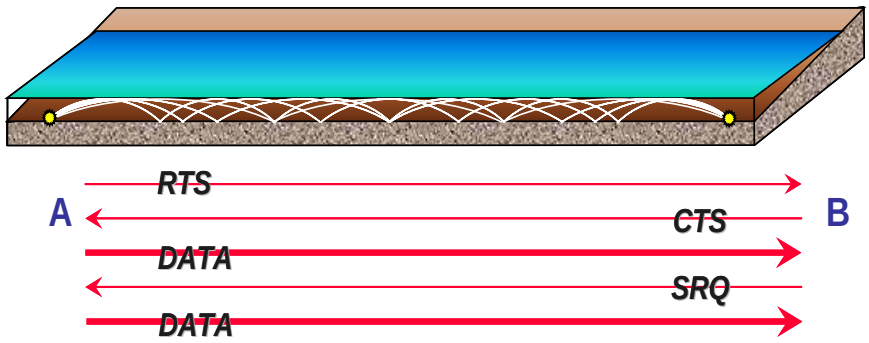

Figure 2. Seaweb node-to-node "Handshaking". [2]

B. RADIO-ACOUSTIC COMMUNICATIONS (RACOM) GATEWAY BUOY

Another component of the Seaweb network is the racom buoy. The buoy is 6 ft long, 3 ft wide, and 3 ft deep and weighs close to 300 lbs. The racom buoy acts as the gateway between the undersea network and the command center at sea or ashore. From shore, a signal can be sent through an Iridium satellite to the buoy. From a nearby boat, a Free Wave radio signal can be sent to the buoy which is then translated into Seaweb packets for transmission to the nodes on the seafloor [1].

Figure 3. Racom Gateway Buoy.

C. SLOCUM GLIDER UUV

Figure 4. Slocum Glider [3,4]

The Slocum Glider is a very unique UUV. While most UUVs can only operate for a few hours, the Glider can operate for up to 30 days and has a range of up to 1500 km on one set of alkaline batteries. It is able to achieve such a long range because it moves through the water column by use of variable buoyancy (Figure 5). The Glider has a 90 watt motor that pumps 504 cc of seawater directly into and out of a short 12mm diameter port on the nose centerline. To control the Glider's angle of attack, it is able to move the battery pack fore and aft (+/- 1") to act as a vernier. While incoming sea water increases the density in the nose and pulls it down, the battery pack's motion controls just how much of an angle is used [3,4].

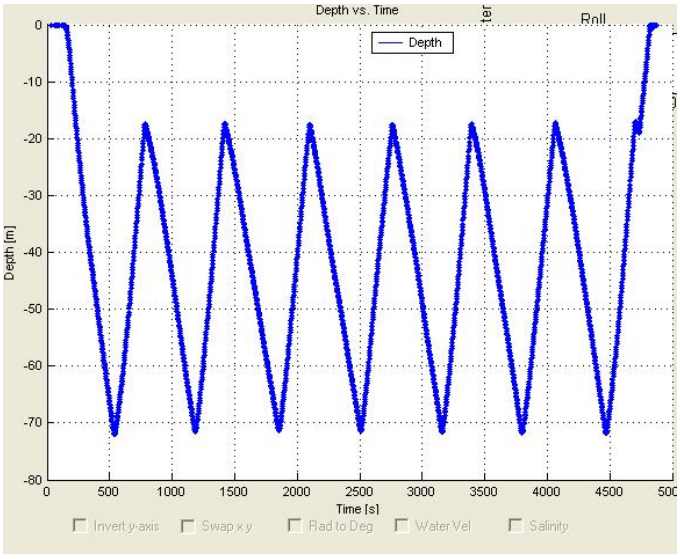

Figure 5. Glider Sawtooth Motion [5].

1. Glider Navigation

The Glider uses Dead Reckoning (DR) to navigate between pre-determined waypoints. When pumping sea water in, the Glider's density becomes greater than that of the surrounding water and it sinks, with the opposite occurring on the return to the surface. To convert this vertical motion into forward motion, the Glider has wings and control surfaces [3,4].

When released for a mission, the glider determines the north/south and east/west distances from its present fix to the next waypoint. On each "yo" maneuver, or vertical dive cycle through the water column, the angle of attack and rate of vertical velocity are used to calculate the forward speed. With periodic surfacing, new GPS fixes permit the Glider to calculate navigation error due to the water currents. The distance between where the Glider thought it was and that of the GPS fix divided by the time of the mission (since the last GPS fix) can give an estimate of the water current. This information is then used as a correction on the next leg of the mission and is factored into the heading and speed necessary to reach the next waypoint [3,4].

2. Sensors/Communications

The Glider has a sensor payload which includes a Conductivity, Temperature, and Depth (CTD) sensor, an additional altimeter, and the GPS and DR sensors. The CTD can be useful for analysis of the water properties in an area. There are two sensors on the

Glider which can give depth readings. The first is a pressure sensor on the CTD (an external sensor), and the second is the altimeter that the Glider uses to calculate vertical velocity. By converting the water pressure to a depth, it can determine its vertical position to an accuracy that is close to 1% [3,4].

The Glider can communicate through a sonar transducer in its nose section, through radio freewave, and also through Iridium satellite. When underwater, the Glider transmits and receives digital communications through its transducer. During the July 2005 Seaweb/Slocum Experiment described in this thesis, the Glider was acoustically commanded to perform acoustic ranging on the deployed underwater network nodes, and telemeter the measured range data back to the dive vessel. This process is discussed in greater depth in Chapter III. When at the surface, the Glider provides information through radio links as to why it surfaced, where it is located, if another waypoint is present for that mission, and the vector to that waypoint [3,4].

THIS PAGE INTENTIONALLY LEFT BLANK

III. SEAWEB/SLOCUM 2005 EXPERIMENTAL OVERVIEW

A. EXPERIMENT OBJECTIVE

To test the effectiveness of Seaweb as a navigation aid for the Slocum Glider, an experiment was conducted in Monterey Bay off the central California coast during July 20-22, 2005. Seaweb nodes were placed on the seafloor at known locations with the racom gateway buoy drifting among them. Experiment personnel were stationed aboard the dive vessel *Cypress Sea*.

As the Glider moved between pre-programmed waypoints in the domain of the deployed Seaweb network, it acoustically ranged the network nodes and sent these range data (Figure 6) to the *Cypress Sea*. The goal of this thesis is to analyze those range data and obtain position fixes that are more accurate than the Glider's DR estimate. In the near future, the hope is that algorithms onboard the Glider will be able to automatically navigate with reasonable accuracy and without ever having to come to the surface for a GPS fix. The long-term goal of this work is to enable a network of fully mobile nodes to position themselves based on their relative locations to each other to clear an area of mines, perform surveys, or conduct other missions as necessary.

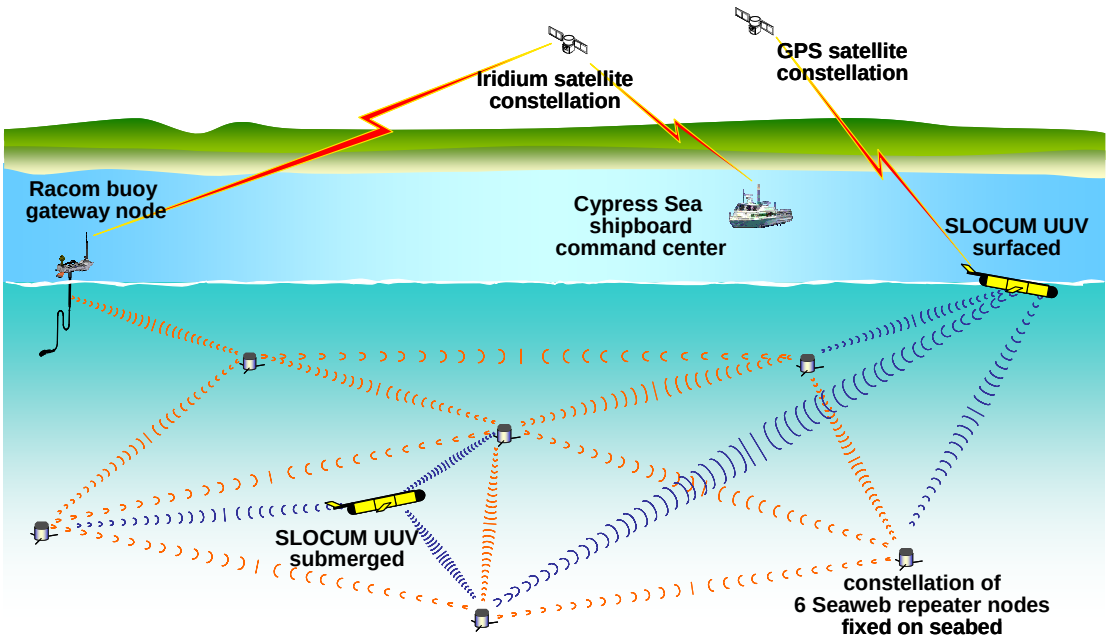

Figure 6. Seaweb/Slocum 2005 Experiment in Monterey Bay [Adapted from 6]

B. SEAWEB/GLIDER COMMUNICATION

1. The "Broadcast Ping"

Through radio communications, the *Cypress Sea* can send Seaweb commands to the racom buoy. Commands addressed for the Glider are forwarded through the Seaweb network to the UUV. The "broadcast ping" command causes the Glider to transmit a utility packet, globally addressing all of the adjacent nodes. These nodes all reply with an "echo" utility packet. Because of the difficulty in receiving several return signals at once, the responding nodes return the echo with a random dwell time. This dwell makes it much more likely that the Glider will receive the echoes without collision. These echoes also report the dwell time, τ, and the Glider compiles and telemeters these range data to the racom buoy which then forwards the packet to the *Cypress Sea* (Figure 7).

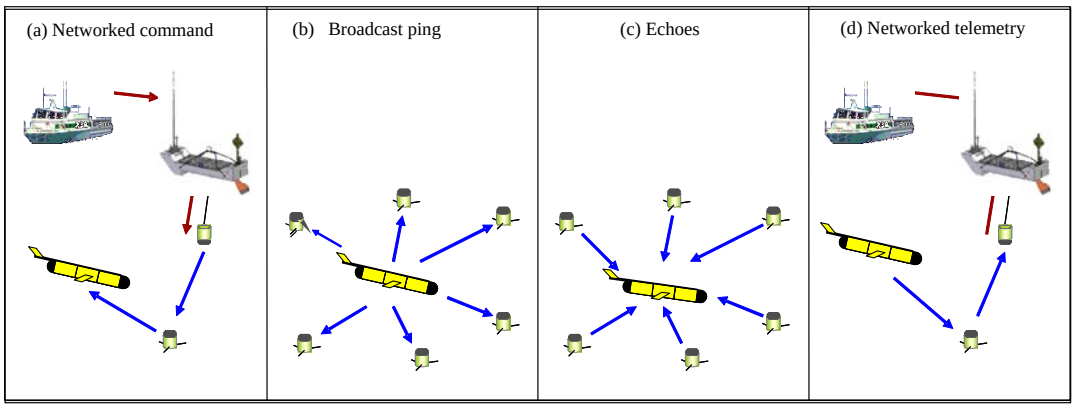

Figure 7. "Broadcast Ping" [Adapted from 6]

2. Calculating the Range

The total elapsed time, from transmission of a ping to the receipt of an echo, is equal to the round-trip propagation plus the dwell time (1). In order to calculate a range from the Glider to each of the nodes, r_{gi}, this total elapsed time (Figure 8) is multiplied by the speed of sound in water, as seen in (2-3). A 1500 m/s assumption is used for this calculation. Because of reciprocity (the fact that a sound wave will take the same path between two points independent of the receiver position), the time that it takes for a pulse to travel from node *i* to the glider is the same as the time that it takes for the pulse to travel along the reverse path. Therefore, the distance from node *i* to the glider calculated from each pulse transit time should be the same, i.e. $d_{ig} = d_{gi}$. Equation (3) expresses the estimated range in terms known at node *g*.

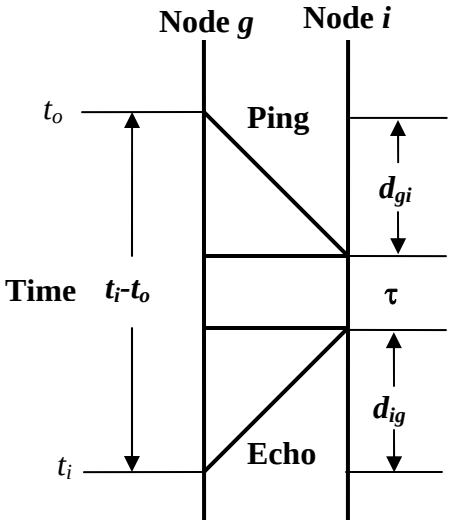

Figure 8. Seaweb Ranging from node *g* to node *i*. [Adapted from 6]

$$t_i - t_o = d_{gi} + \tau + d_{ig} \tag{1}$$

$$r_{gi} = 1500\frac{m}{s} \cdot \left(\frac{d_{gi} + d_{ig}}{2} \right) \tag{2}$$

$$r_{gi} = 1500\frac{m}{s} \cdot \left(\frac{t_i - t_o - \tau}{2} \right) \tag{3}$$

A shorthand notation used in the remaining chapters omits the subscript for the Glider, $r_i = r_{gi.}$

THIS PAGE INTENTIONALLY LEFT BLANK

IV. DESIGNING AN ALGORITHM TO TRACK THE GLIDER

A. KNOWN PARAMETERS

Seafloor node positions and their ranges from the Glider at each fix are the known parameters. The distance between two nodes and the ranges between those two nodes and the Glider form three sides of a triangle. Since the ranges can only meet at two distinct points, the Glider's position can be narrowed down to those two possibilities (Figure 9). By obtaining those two solutions, though, from several node pairs, the ambiguity may be resolved as demonstrated in Figure 10.

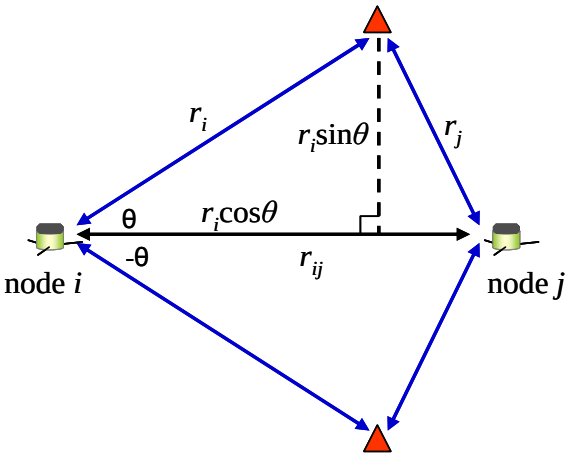

Figure 9. Finding 2 Possible Solutions With 3 Known Sides of a Triangle. [From 6]

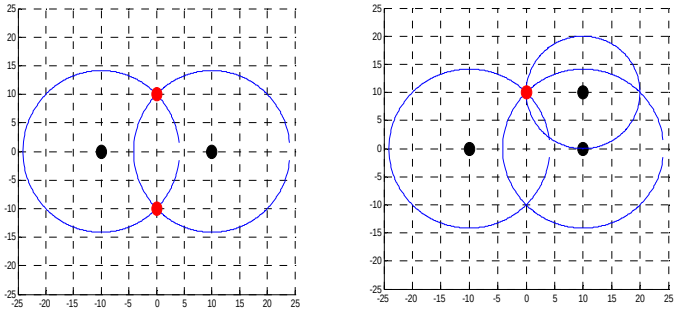

Figure 10. Range Circles for 2 and 3 Nodes.

B. REAL WORLD COMPLICATIONS WITH ERROR

Since measured ranges are imperfect, a more complicated method of positioning is required. Not all range circles, as in Figure 11, are likely to meet at one point since the range will have some error. This is expressed in equation 4 where r is the measured range, Δr is the range uncertainty, and R is the interval of possible ranges. Finding the two intersections of each circle (each pair of solutions for two nodes) can lead to an estimated position. By looking at Figure 11, one can see that the Glider position would be close to the cluster of red dots that represent the circle intersections.

$$R = r \pm \Delta r \tag{4}$$

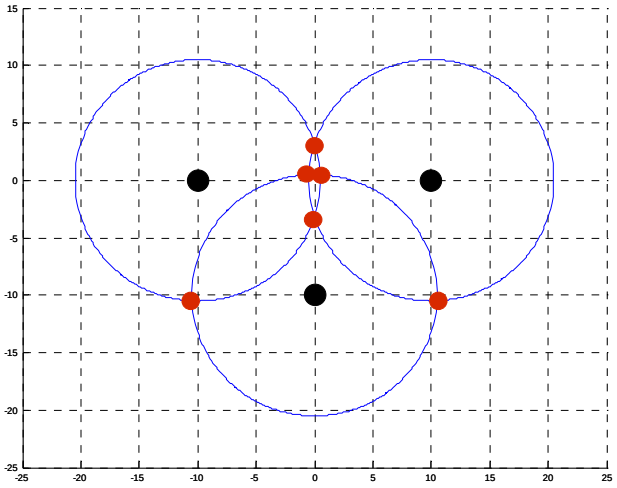

Figure 11. Solutions With Error.

C. ACCOUNTING FOR THE THIRD DIMENSION

To make the range data more accurate and easier to work with, the geometry can be projected onto the x-y plane. Since the seafloor is not flat, the depths of the Seaweb nodes must be taken into consideration when calculating the distance between pairs of nodes (Figure 12) and (5-7).

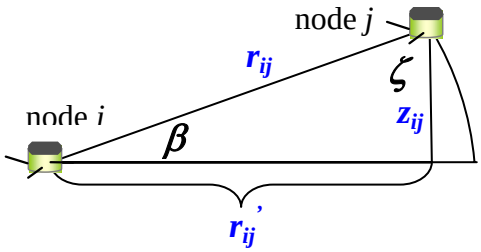

Figure 12. Transforming Node Distances to a Common x-y Plane.

$$x_{ij} = x_j - x_i$$
$$y_{ij} = y_j - y_i \quad (5)$$
$$z_{ij} = z_j - z_i$$

$$r_{ij} = \sqrt{x_{ij}^{\,2} + y_{ij}^{\,2} + z_{ij}^{\,2}} \quad (6)$$

$$r_{ij}' = \sqrt{x_{ij}^{\,2} + y_{ij}^{\,2}} = \sqrt{r_{ij}^{\,2} - z_{ij}^{\,2}} \quad (7)$$

Since the Glider makes full use of the water column as it moves through the network, its depth must also be considered. The Glider can send its depth, along with the range data, to the command center. While this was not done in the July test, future tests can incorporate it. Without this known depth, calculations are more difficult and much less accurate. Figure 13 demonstrates the error present without this known value for two nodes displaced in depth by 100 m. At horizontal ranges close to zero, the true range from the Glider to the node is close to 100 m (very high error between the two). To decrease the error between the true range (r_{ij}) and the horizontal range (r_{ij}') to 1%, the Glider would need to be at a horizontal range of 707 m.

To calculate the horizontal range to the Glider, projection similar to that of Figure 12 is depicted in Figure 14. Equations 8 and 9 show that, through the Pythagorean Theorem, the horizontal range from node *i* (r_i') or node *j* (r_j') is calculated simply from the true range to the glider (r_i or r_j) and the height difference of the glider (z_g). z_g' is the depth of the Glider and z_i is the depth of node *i*.

$$z_g = \left| z_g' - z_i \right| \quad (8)$$

$$r_i' = \sqrt{r_i^2 - z_g^2}$$
$$r_j' = \sqrt{r_j^2 - z_g^2} \tag{9}$$

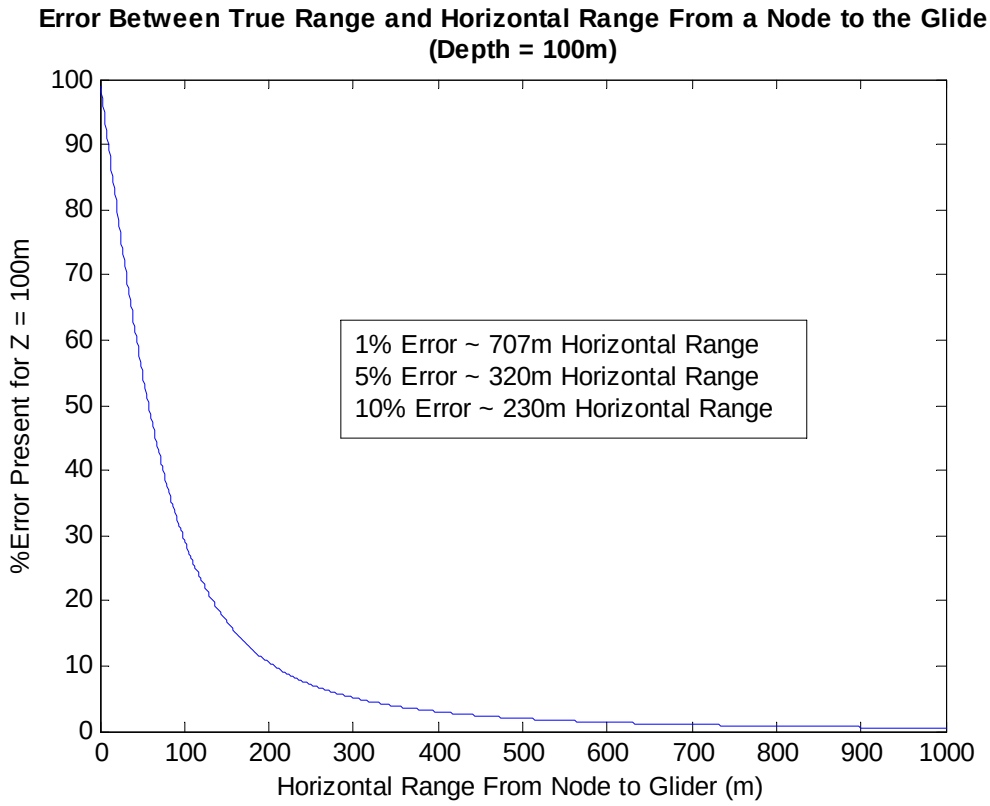

Figure 13. Range Estimation Error for 100 m Depth Uncertainty of Target Node

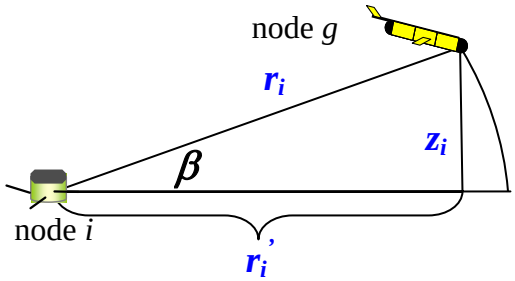

Figure 14. Transforming Ranging Data to a Common X-Y Plane

D. FINDING THE GLIDER POSITION

As mentioned earlier, each pair of nodes that have good ranges to the Glider will generally produce two possible solutions. In most cases, one of these solutions will be correct and one will not.

The node positions on the seafloor and the ranges from the Glider to each node are known. The projected ranges from all nodes to all other nodes are calculated (r_{ij}'), as well as the horizontal distance to the Glider from each node (r_i' or r_j'). All ranges have now been transformed onto a common x-y plane.

From these ranges, further calculations lead to the position of each pair of solutions for two given nodes. The first calculation involves the angle between a node's horizontal axis and the other node it is being paired with, called phi (ϕ) (Figure 15). Since ϕ' is the angle with respect to the horizontal axis, special considerations must be made when calculating ϕ outside of the first quadrant. This is illustrated in Figure 16 and (10-11). This will lead to ϕ being defined as an angle between 0 and 360°.

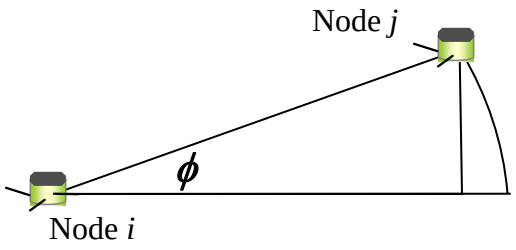

Figure 15. Calculating the Angle Phi

$$\varphi' = \tan^{-1}\left|\frac{y_i - y_j}{x_i - x_j}\right| \tag{10}$$

$$\varphi = \begin{Bmatrix} \varphi' & x_i \langle x_j, y_i \le y_j \\ \pi - \varphi' & x_i \rangle x_j, y_i \le y_j \\ \varphi' + \pi & x_i \rangle x_j, y_i \ge y_j \\ -\varphi' & x_i \langle x_j, y_i \ge y_j \end{Bmatrix} \tag{11}$$

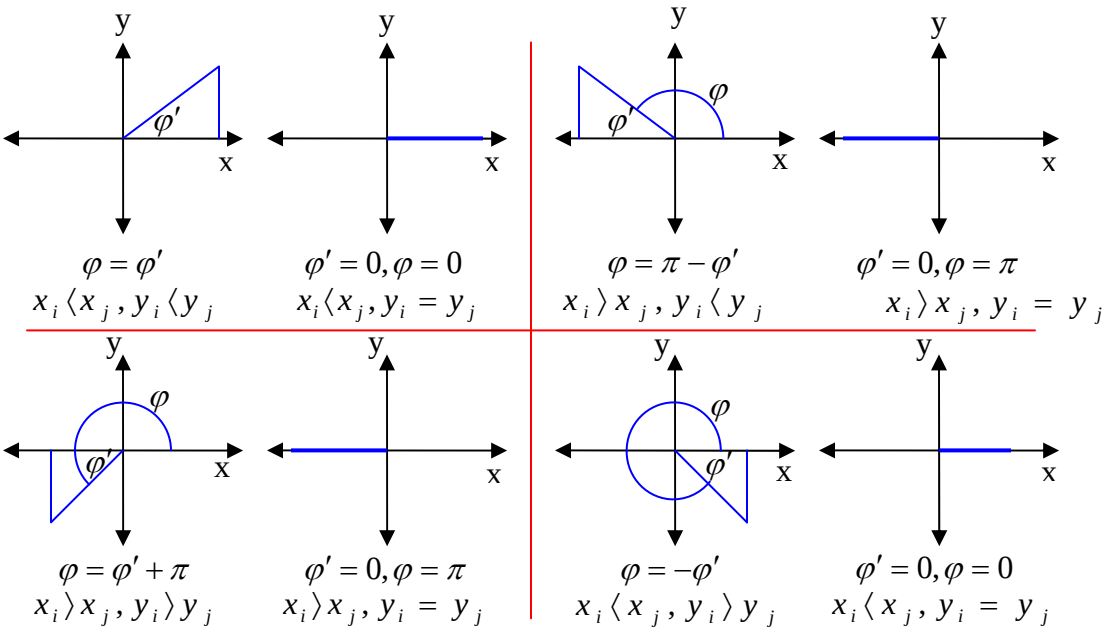

Figure 16. ϕ Defined For All Combinations of x-y Coordinates of Two Nodes [Adapted from 6].

In special cases where nodes *i* and *j* have the same x coordinate, ϕ' will be the arctangent of 0, which is infinite. Therefore, ϕ must be defined for this special case as either π/2 or 3π/2 (Figure 17 and (12)).

$$\varphi = \begin{cases} \frac{\pi}{2} & x_i = x_j, y_i \langle y_j \\ -\frac{\pi}{2} & x_i = x_j, y_i \rangle y_j \end{cases} \qquad (12)$$

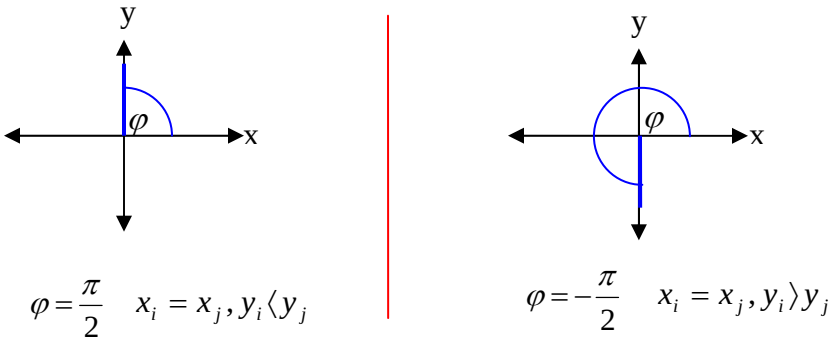

Figure 17. Two Nodes With Same x Coordinate [Adapted from 6].

The next angle of importance is the angle between the line connecting two nodes of interest and the line between node i and the Glider. This will be called θ. In order to calculate θ, the Law of Cosines (Figure 18 and (13)) must be used since all 3 sides of the triangle are known without any known angles.

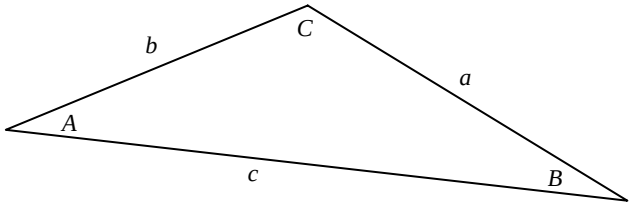

Figure 18. The Law of Cosines.

$$c^2 = a^2 + b^2 - 2ab \cdot \cos(C)$$
$$C = \cos^{-1}\left(\frac{c^2 - a^2 - b^2}{-2ab}\right) \tag{13}$$

The final angle used to find the positions of the solutions is named γ. γ_a is the addition of ϕ and θ for one solution and γ_b is the subtraction of θ from ϕ for the other solution (Figure 19 and (14)).

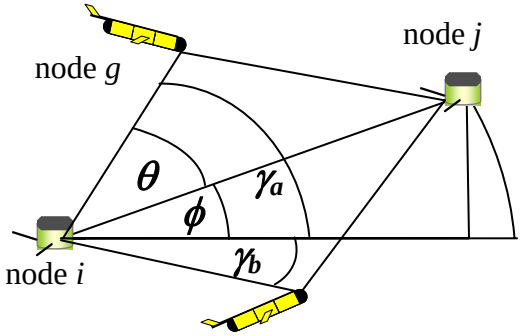

Figure 19. Two Possible Values for γ Leading to Two Possible Solutions.

$$\gamma = \varphi \pm \theta \tag{14}$$

Figure 20 illustrates a summary of the angles ϕ, θ and γ given two node positions and ranges to the Glider. Only one Glider solution is shown in the figure, but two are present as stated earlier. Also illustrated in Figure 20 are the distances between nodes along with the distances from the nodes to the Glider. All calculations are made with respect to a central node at (0,0).

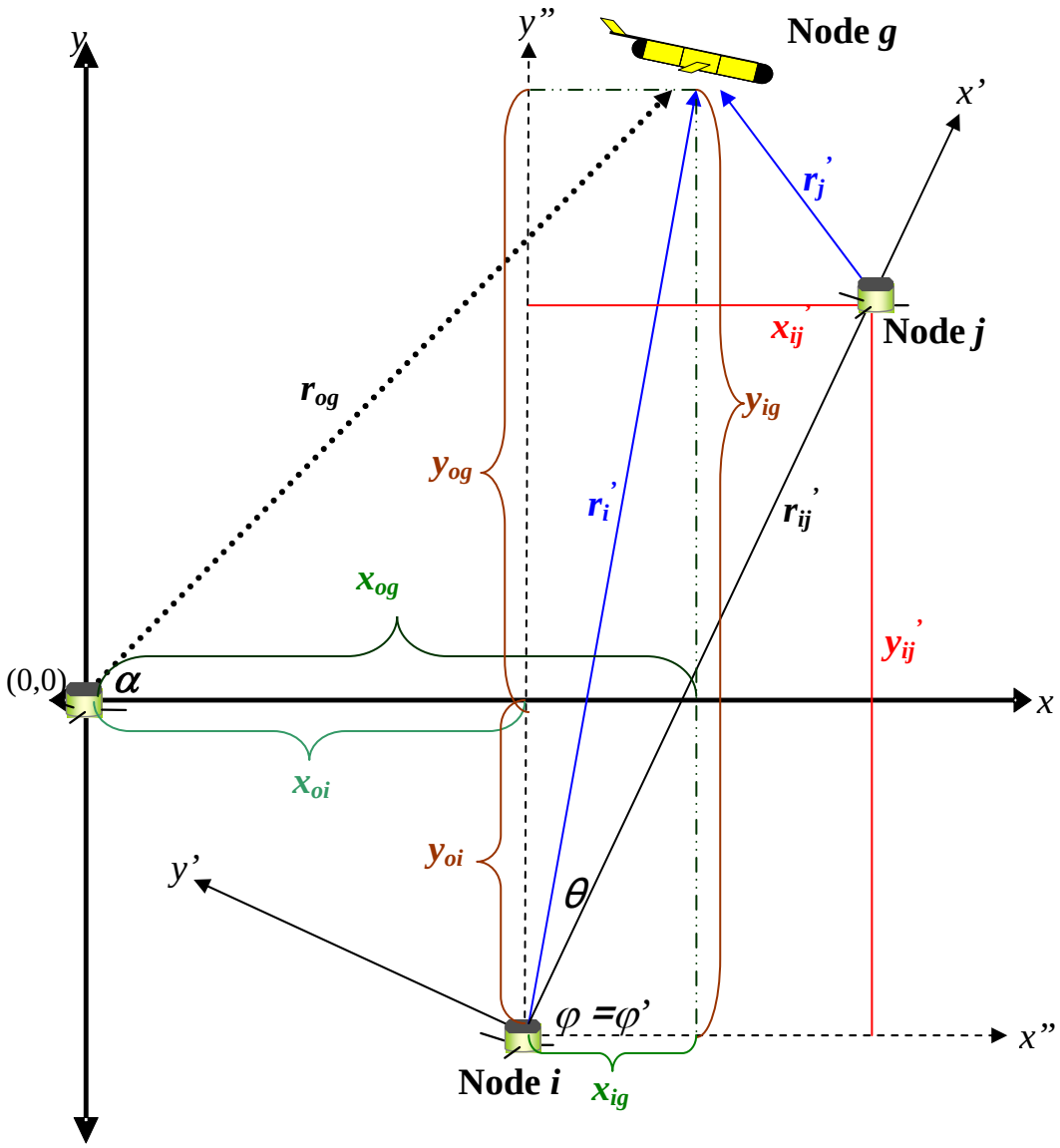

Figure 20. Coordinate Transformations in x-y Plane of Two Nodes.

For the situation illustrated in Figure 20, several calculations can be made. Since this situation refers to the first quadrant (with node *i* as the reference node), ϕ is equal to ϕ’ (10 and 11). The Law of Cosines allows for the calculation of θ (13). These two angles together give the two possible solutions for γ (14). Once γ has been calculated, the *x* and *y* differences between node *i* and the Glider (x_{ig} and y_{ig}, respectively) can be calculated with (15). Since all node positions are given in reference to the central node, the *x* and *y* differences from the central node to each node (x_{oi} and y_{oi}) is simply the *x* or *y* position of

that node (16). Finally, the addition of those two *x* and *y* differences leads to a final solution for that pair of nodes (17).

$$x_{ig} = r_i' \cos(\gamma)$$
$$y_{ig} = r_i' \sin(\gamma) \tag{15}$$

$$x_{oi} = x_i$$
$$y_{oi} = y_i \tag{16}$$

$$x_{og} = x_{oi} + x_{ig}$$
$$y_{og} = y_{oi} + y_{ig} \tag{17}$$

Figure 21 shows every possible solution as a red circle with the true position given in solid red. Node positions are given as open squares.

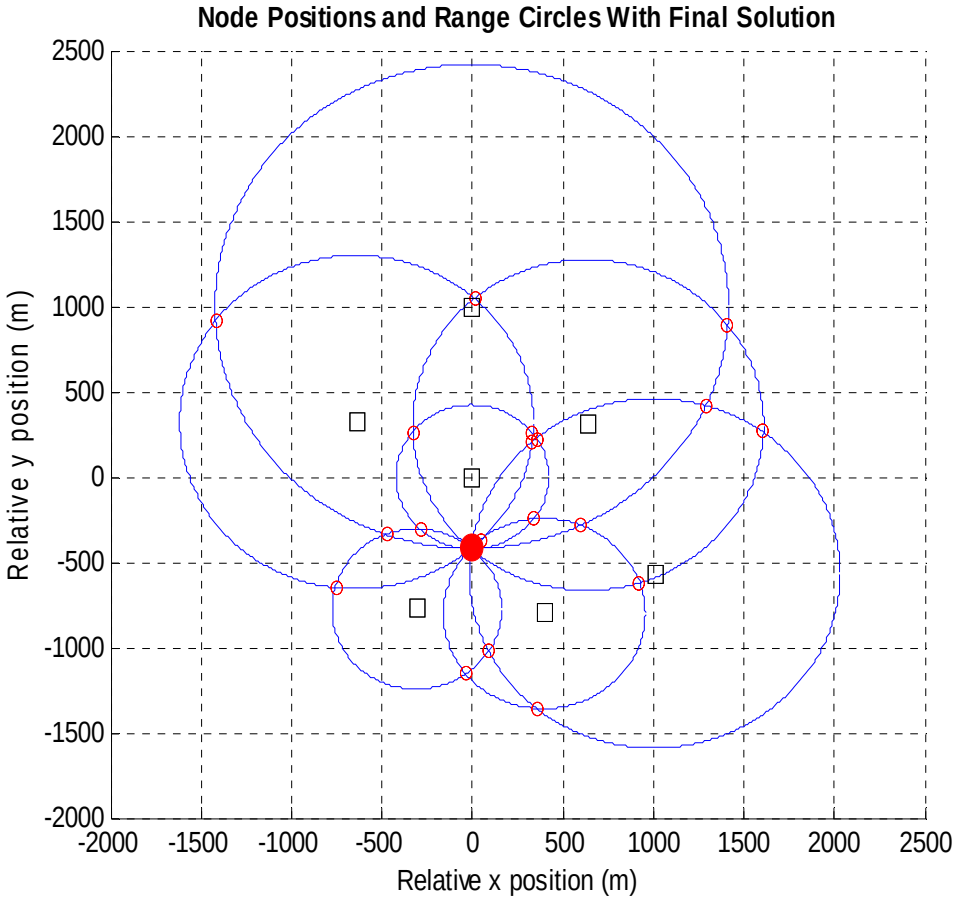

Figure 21. Node Positions and Range Circles to the Glider

E. FINDING A SOLUTION WITH ERROR-PRONE DATA

1. Non-intersecting Circles

Since the data that will be used in the experiment are not perfect, a special case must be considered, which involves the situation where two circles do not intersect. If the Glider is between two nodes and the ranges have an error such that the distance between the two nodes is greater than the sum of the two ranges (18), an extra calculation is made. Since, in this situation, the Glider is most likely collinear with the two nodes, a possible solution that is between the nodes will be somewhat accurate. To find that position, the ranges from node *i* to node *j* with the subtraction of the two ranges from each node to the Glider gives a value named *e* (19). Taking half of that *e* value and adding it to the range from node *i* to the Glider will give a range that is along the line between the two nodes (Figures 22 and 23 and (20)). Equation 21 gives that solution's x and y position.

$$r_{ij} \rangle r_i + r_j \tag{18}$$

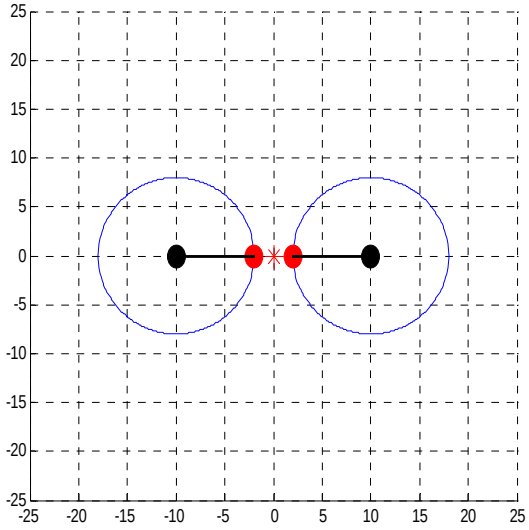

Figure 22. The Case of Non-Intersecting Spheres.

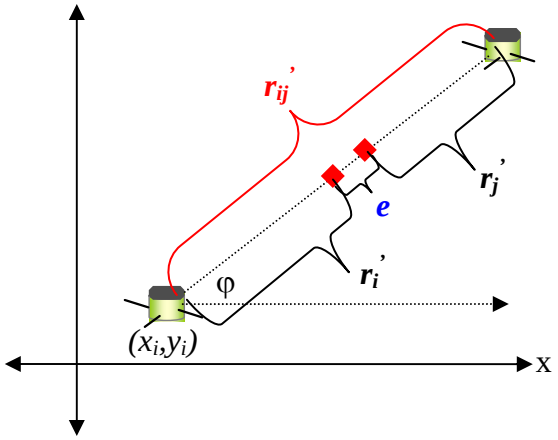

Figure 23. Another View of Non-Intersecting Geometry [Adapted from 6].

$$e = r_{ij}' - r_i' - r_j' \tag{19}$$

$$\frac{1}{2}e + r_i' = r_e \tag{20}$$

$$\begin{aligned} x_{og} &= x_{oi} + r_e \cdot \cos\varphi \\ y_{og} &= y_{oi} + r_e \cdot \sin\varphi \end{aligned} \tag{21}$$

2. Geometric Dilution of Precision

It is also important to note that the angle from the Glider to both of the nodes will affect the accuracy of the good solution. A very shallow angle (Figure 24A) will lead to more error than that seen in Figure 24B. Figure 24B shows that this configuration can tolerate more range error. This is known as Geometric Dilution of Precision [7].

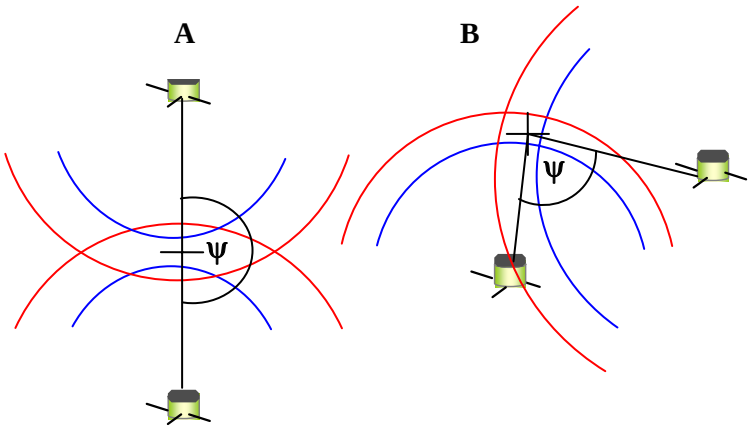

Figure 24. Geometric Dilution of Precision [Adapted from 7].

F. TWO LOCALIZATION ALGORITHMS

The total number of possible solutions for a set of seven nodes is 42. With perfect data, half of these 42 solutions coincide with the position of the glider and the other half are false solutions at the other intersections of the circle pairs. For real data that have some inherent error, though, nearly none of those points will be absolutely correct. Half will, however, be very close to each other, as illustrated in Figure 25. The left figure shows range data that have some small error. When the figure is zoomed in, none of the points appear to be directly on the Glider's true position (red triangle). Accounting for all of the 42 points, however, will lead to an estimated position.

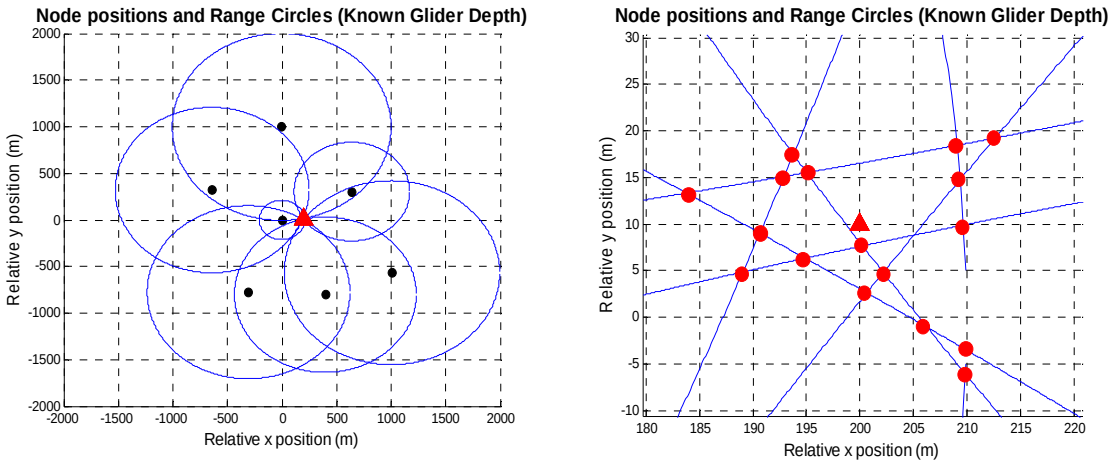

Figure 25. Several Possible Solutions.

1. The Weighting Method

ENS Matthew Hahn's Master's Thesis titled *Undersea Navigation Via a Distributed Acoustic Communications Network* looked at similar range data from a Seaweb network to the ARIES UUV. To determine position from all of the possible solutions, he assigned weight values to each individual solution. A solution's weight value depended on its proximity to all of the other solutions. Therefore, a tight cluster of solutions arising from range data with little error would be given high weights and any outlying solutions would have small weights [6].

In a seven node system with 42 solutions, the weight of the first solution is calculated by taking the inverse of its distance from the second solution and raising it to a power, κ (22). That first solution is then compared to the third, fourth and so on up to the

42^{nd} solution to get a total weight for that point (23). In case two solutions happen to lie directly on each other (which would occur with error-free data), a correction factor, *C*, is added. Without this, equation 22 would show a division by 0. The correction factor used in his thesis was .01 giving that point a weight of 100. ENS Hahn also found that a value of $\kappa = 1$ gave the best results. The last step in determining the final position based on the weighting method involves taking each point's fraction of total weight and multiplying it by that solution's x and y value (24). When every solution's weight is summed together, the final position is determined [6].

$$W_k = \sum_{a=1,b=1,a\neq b}^{m} \left[\frac{1}{(x_a - x_b)^2 + (y_a - y_b)^2 + C} \right]^{\kappa} \tag{22}$$

$$W_{total} = \sum_{k=1}^{n} W_k \tag{23}$$

$$\begin{aligned} x_{est} &= \sum_{k=1}^{n} \frac{W_k}{W_{total}} x_k \\ y_{est} &= \sum_{k=1}^{n} \frac{W_k}{W_{total}} y_k \end{aligned} \tag{24}$$

2. The Center-of-Mass Method

This thesis introduces a new method, called the center-of-mass method, for estimating the Glider position. In this method, all of the solutions' x and y values are averaged to yield a center of mass for the system (25 and 26). Since each pair of nodes will have a solution that is correct and a solution that is wrong, throwing out the incorrect solutions will lead to a much better approximation of the Glider position. To do this, each solution's distance from the center of mass is calculated ($dist_{sola}$, $dist_{solb}$) (27). Of the two solutions that are present for a pair of nodes, the solution farther from the center of mass is then discarded (28 and 29). With perfect data, this gives the exact solution, but with range errors present, some of the incorrect solutions may have been chosen. To further improve the final solution, a new center of mass is then taken from the 21 positions chosen in the first iteration (30). Comparing the positions of each pair to this new center

of mass is intended to throw out more of the incorrect points (31-33). The final position (x_{final}, y_{final}) is then taken from the mean of all 21 of these new solutions (34).

$$\begin{aligned} sola &= (x_a, y_a) \\ solb &= (x_b, y_b) \end{aligned} \tag{25}$$

$$\begin{aligned} cmx &= \frac{\sum_{a=1}^{n} x_a + \sum_{b=1}^{n} x_b}{2n} \\ cmy &= \frac{\sum_{a=1}^{n} y_a + \sum_{b=1}^{n} y_b}{2n} \end{aligned} \tag{26}$$

$$\begin{aligned} dist_{sola} &= \sqrt{\left|x_a - cmx\right|^2 + \left|y_a - cmy\right|^2} \\ dist_{solb} &= \sqrt{\left|x_b - cmx\right|^2 + \left|y_a - cmy\right|^2} \end{aligned} \tag{27}$$

$$\begin{aligned} x_{new} &= x_a \\ y_{new} &= y_a \end{aligned} \quad dist_{sola} \le dist_{solb} \tag{28}$$

$$\begin{aligned} x_{new} &= x_b \\ y_{new} &= y_b \end{aligned} \quad dist_{solb} \langle dist_{sola} \tag{29}$$

$$\begin{aligned} cmx_{new} &= \frac{\sum_{c=1}^{n} x_{new}}{n} \\ cmy_{new} &= \frac{\sum_{c=1}^{n} y_{new}}{n} \end{aligned} \tag{30}$$

$$\begin{aligned} dist_{sola}' &= \sqrt{\left|x_a - cmx_{new}\right|^2 + \left|y_a - cmy_{new}\right|^2} \\ dist_{solb}' &= \sqrt{\left|x_b - cmx_{new}\right|^2 + \left|y_b - cmy_{new}\right|^2} \end{aligned} \tag{31}$$

$$\begin{aligned} x_{new}' &= x_a \\ y_{new}' &= y_a \end{aligned} \quad dist_{sola}' \le dist_{solb}' \tag{32}$$

$$\begin{aligned} x_{new}' &= x_b \\ y_{new}' &= y_b \end{aligned} \quad dist_{solb}' \langle dist_{sola}' \tag{33}$$

$$x_{final} = \frac{\sum_{c=1}^{n} x_{new}'}{n}$$
$$y_{final} = \frac{\sum_{c=1}^{n} y_{new}'}{n} \quad (34)$$

THIS PAGE INTENTIONALLY LEFT BLANK

V. TESTING WITH SIMULATION

A. SIMULATION ONE: 40,000 POINTS

To test the effectiveness of both algorithms, a Monte Carlo simulation was performed. This simulation generated 40,000 random Glider positions within a 2 km by 2 km by 100 m region. The simulated space encompassed the actual seafloor nodes as deployed in the July experiment. Exact ranges from the 40,000 Glider positions to the seven seafloor nodes were calculated and are assumed to be error-free.

1. Testing Both Methods with Error-Free Ranges

To ensure that the MATLAB program was written correctly for both positioning methods, the simulation was run 40,000 times with error-free ranges. The error-free runs demonstrate how effective the algorithms are in finding the true position. Positioning errors are calculated to give a quantitative comparison of the two algorithms. The errors are expected to be very low, and with a perfect algorithm, it would be zero every time. Figures 26 and 27 demonstrate these results. It must be noted that the scales of the x axes are different for both graphs. Also, there are many points at an error of ~0 m, but the y-axes scales are clipped to make the graphs a bit clearer. It must be noted that the histogram for the weighting method appears to have much fewer total occurrences because there are so many results at or very close to 0 m.

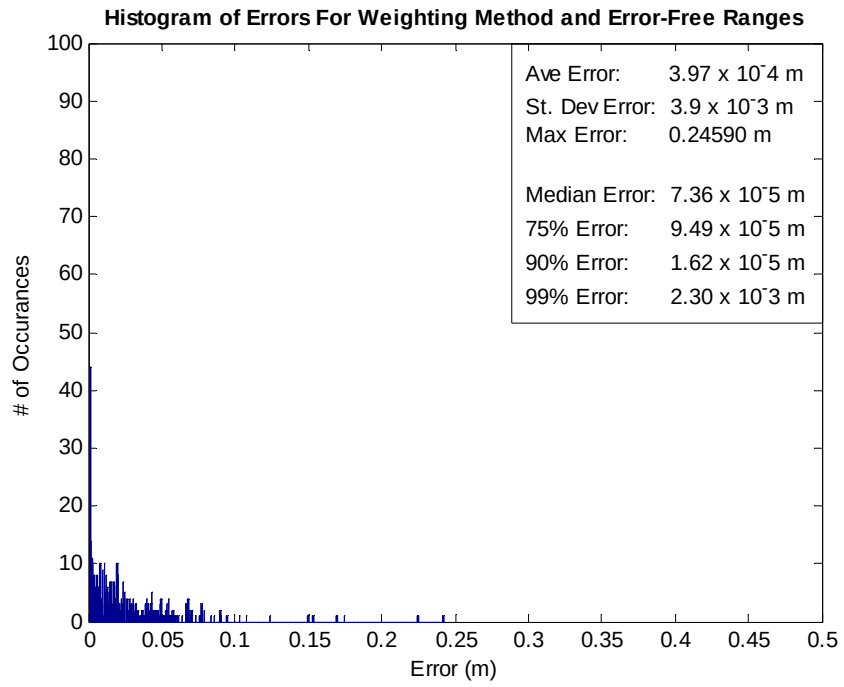

Figure 26. Simulation One Using the Weighting Method and Error-Free Ranges

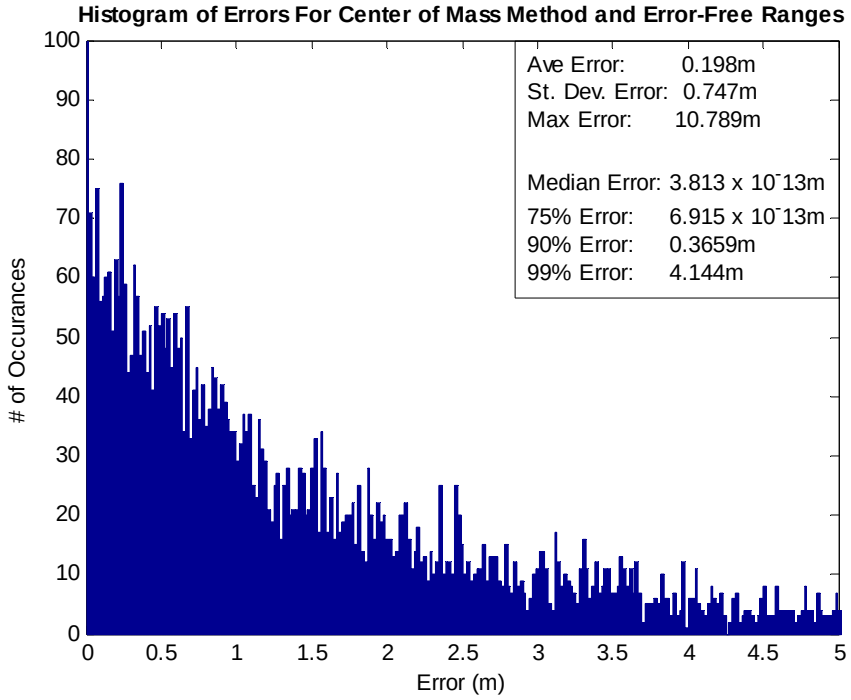

Figure 27. Simulation One Using the Center-of-Mass Method and Error-Free Ranges

The results in Figures 26 and 27 demonstrate that both algorithms have been written correctly. The weighting method appears to be the better of the two based on maximum and average error. The center-of-mass method does, however, calculate a nearly perfect Glider position at least 75% of the time. The center-of-mass method does, however, appear to have some flaws close to 25% of the time. In order to understand the reason for these flaws, the program must be analyzed. Figure 28 attempts to explain the reason for the failure of the center-of-mass method for nearly ¼ of the Glider positions. It appears as though a Glider position that is at the outer reaches of the Seaweb network leads to these errors. As shown in Figure 28, the set of small red circles represents every solution point for each pair of nodes. Notice that there is a large cluster of these circles close to the Glider position of (727, 976). The small red cross at (335, 391) is the position of the center of mass of all of the solutions. Since the Glider is near the northeastern edge of the network, the large ranges from the nodes toward the southwest of the network lead to some solutions which are quite far away from the true position. After throwing out these incorrect points and taking the center of mass again, a new solutions is found to be at the position (739, 973), which is much closer to the true Glider position.

While this particular simulation (with no range error) appears to favor the weighting method, the same simulation will be tested with range errors of +/- 10 m. After gathering the data from that simulation, the more favorable method will be chosen for the rest of the analysis.

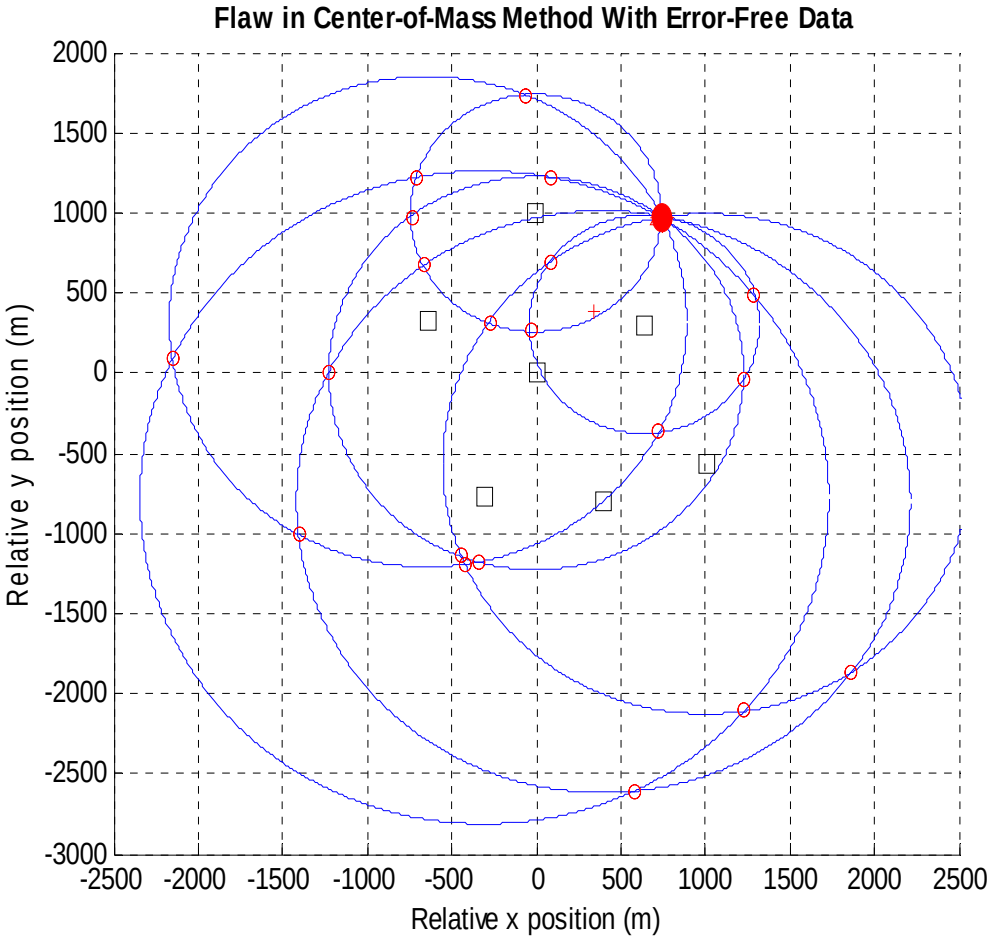

Figure 28. Circumstance Where Center of Mass Method Has Difficulty Computing the Correct Glider Position When No Range Error is Included

2. Simulation One With +/-10m Range Error Added

With a +/-10 m range error added to the simulation, both are again tested for effectiveness. This test will truly show the better method, since real range data always have some inherent error. In Figure 29, a histogram has again been made from each of the 40,000 errors for the weighting method. Figure 30 shows a similar histogram for the center of mass method.

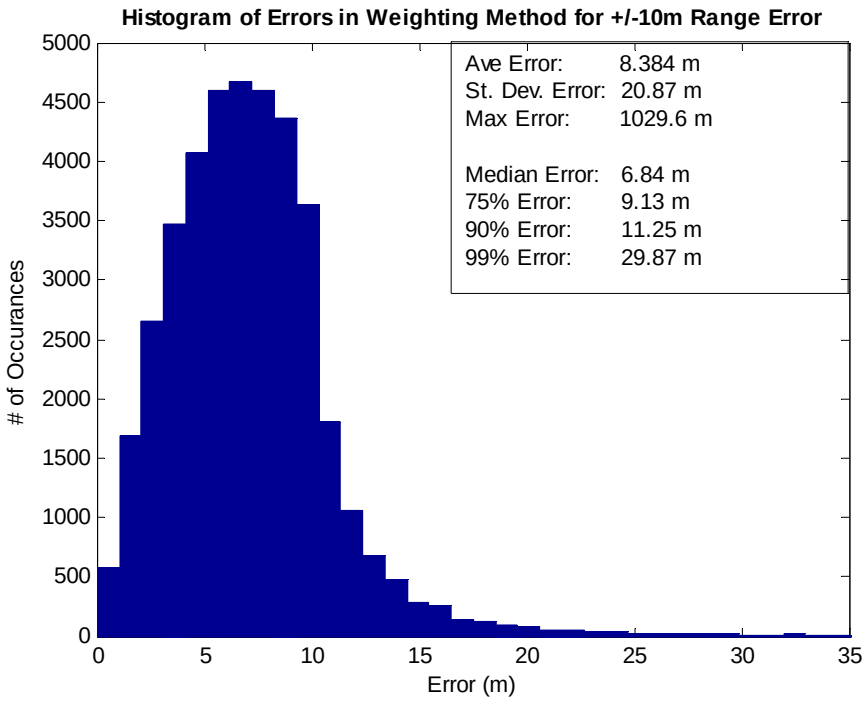

Figure 29. Simulation One Using the Weighting Method and a +/-10 m Range Error

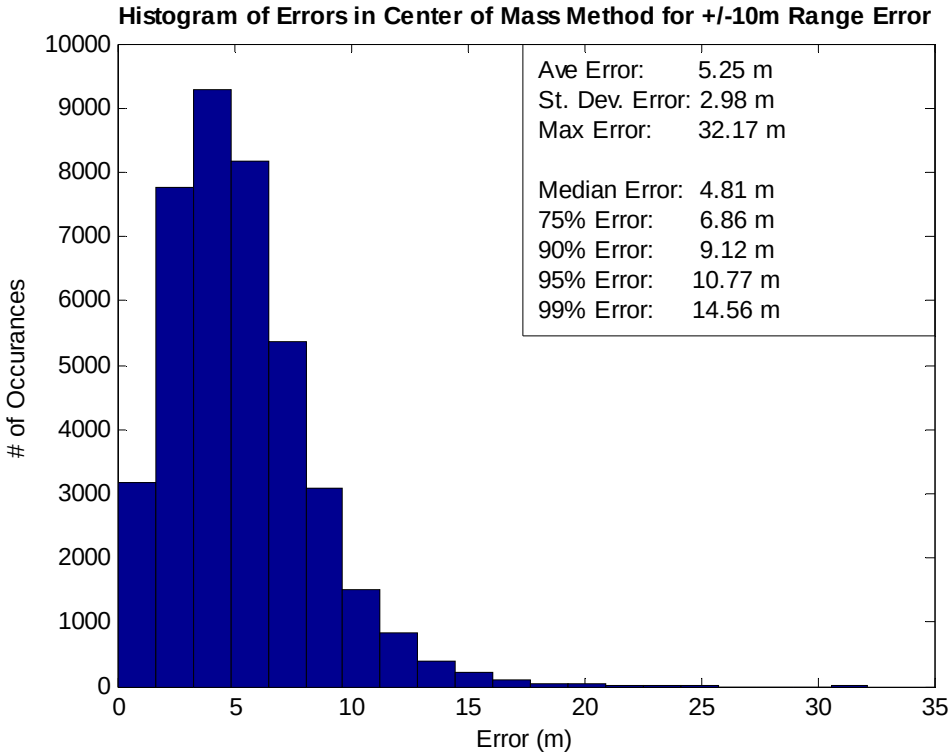

Figure 30. Simulation One Using the Center-of-Mass Method and a +/-10 m Range Error

As seen in the results from Figures 29 and 30, the center-of-mass method has proven to be the superior method for range data that are subject to some error. The center-of-mass method resulted in an average error of 5.25 m compared to 8.38 m for the weighting method. All other categories including the standard deviation and maximum errors were also lower for the center-of-mass method. The weighting method weakens when error is present because usually no two solutions lie directly on the same point. It is also possible that a cluster of solutions can be present at another location. The center-of-mass method, therefore, has outperformed the weighting method and is the only method used in the remainder of this thesis.

A special case is considered (Figure 31). Here, several possible solution points lie close to the true Glider position (blue circle). The range error, though, has caused another cluster of solutions to gather close to the red triangle, which is the position given by the weighting method. Since two of those points are closer together than any other two solutions, their weights are amplified higher than any other solutions' weights, leading to a positioning error of 32 m.

The same case is tested with the center of mass method as a comparison. By properly neglecting the incorrect solutions, this method was able to calculate an error of 0.9m, as illustrated in Figure 32. This again demonstrates the improvement that the center-of-mass method makes in tracking the Glider.

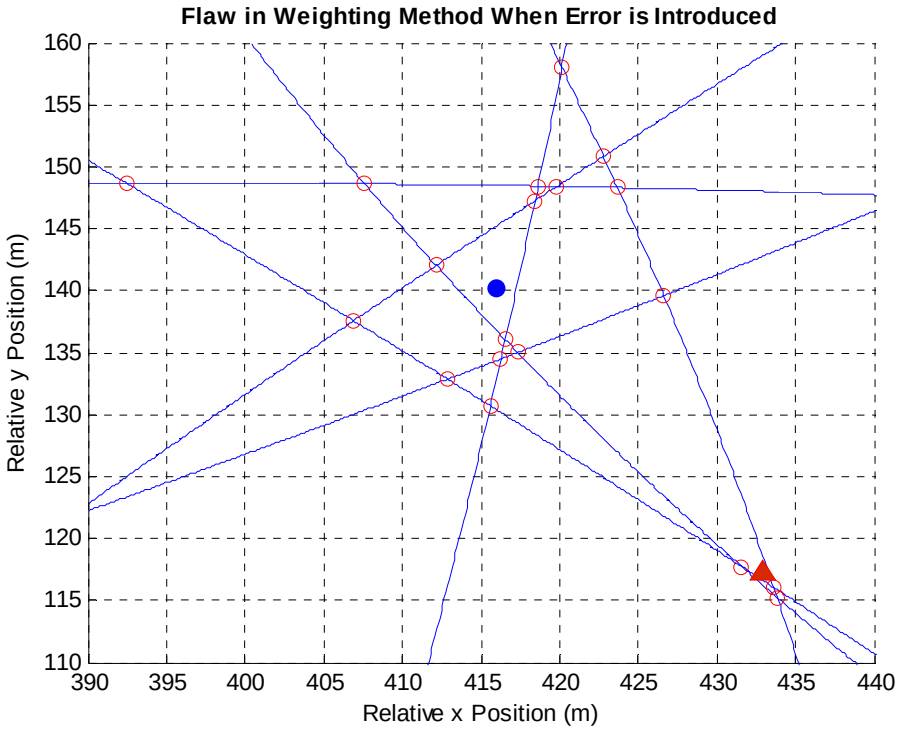

Figure 31. Circumstance Where Weighting Method Has Difficulty Computing the Correct Glider Position When Range Error is Included

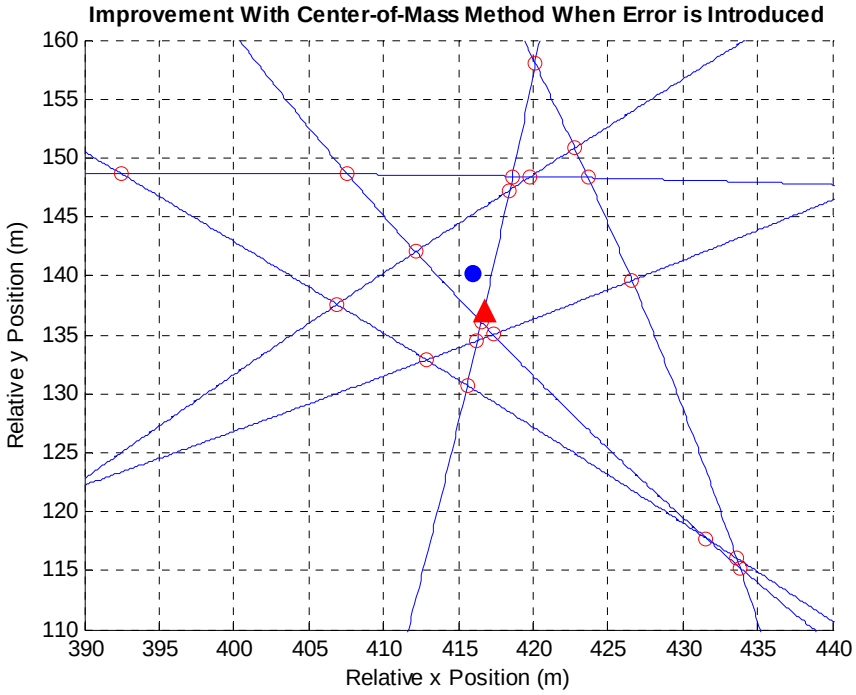

Figure 32. Improvement with Center of Mass Method

B. SIMULATION TWO: TWO SAMPLE TRACKS

In simulation two, two circular tracks are defined as hypothetical Glider tracks. The first track has a radius of 600 m, centered at the origin (Figure 33). The second track has a radius of 1200 m with the same center (Figure 34). These two tracks should illustrate the dependence on Glider position for the center-of-mass method's ability to track the Glider. As seen in Section A, Part 1 of this chapter, a closer Glider position to the center of the network leads to more accuracy in tracking. The track around the periphery of the network tends to suffer greater geometric dilution of precision, and hence the estimated track accuracy is less than that of the inner track.

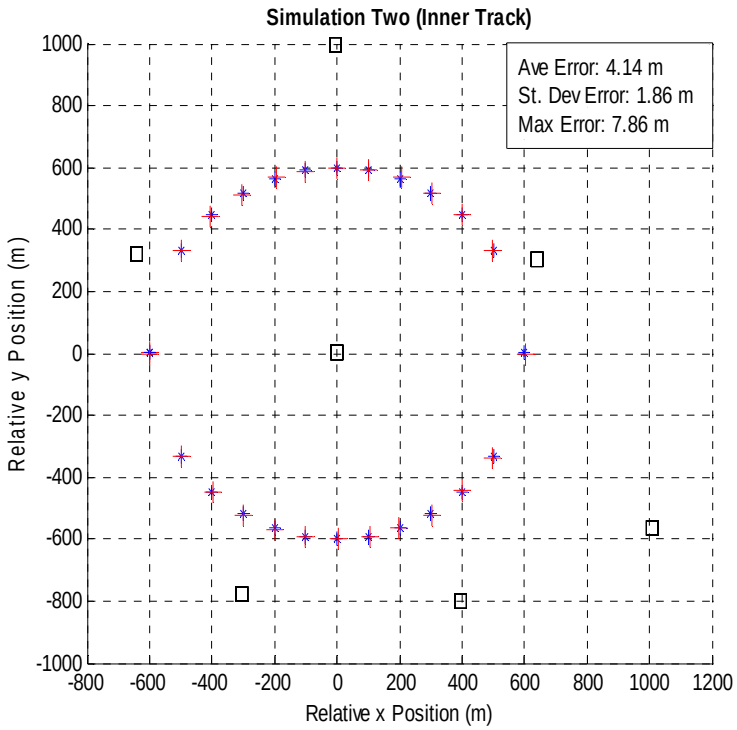

Figure 33. Simulation Two: Inner Track

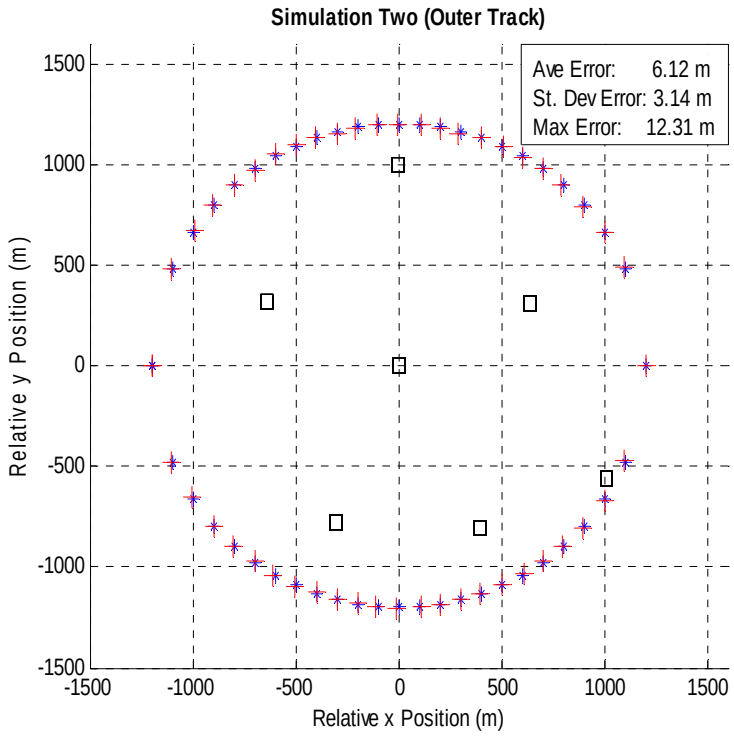

Figure 34. Simulation Two: Outer Track

Figures 33 and 34 illustrate that accuracy does, in fact, depend on Glider position. As shown in figure 33, the average error for the inner track was 4.14 m with a standard deviation of 1.86 m and a maximum error of 7.86 m. The outer track showed an average error of 6.12 m with a standard deviation of 3.14 m and a maximum error of 12.31 m. The red crosses represent the Glider's true position and the blue asterisks are the positions of the Glider from the algorithm. Now that the algorithm has been validated with synthetic range data, it is ready for field testing with real data from Monterey Bay.

THIS PAGE INTENTIONALLY LEFT BLANK

VI. JULY 2005 SEAWEB/SLOCUM EXPERIMENT

A. EXPERIMENTAL SET-UP

The July 2005 Seaweb/Slocum Experiment was a follow-on to the May 2005 Seaweb/ARIES Experiment. In the ARIES experiment, a different UUV was used in the same manner as the Glider: to ping the network, calculate ranges and be tracked. Unlike the Glider, the ARIES UUV operated only near the sea surface. Therefore, the ARIES experiment was performed near shore in shallow water.

Since the Glider uses so much of the water column as it conducts a mission, the July experiment occurred in a deeper part of the Bay (Figure 35).

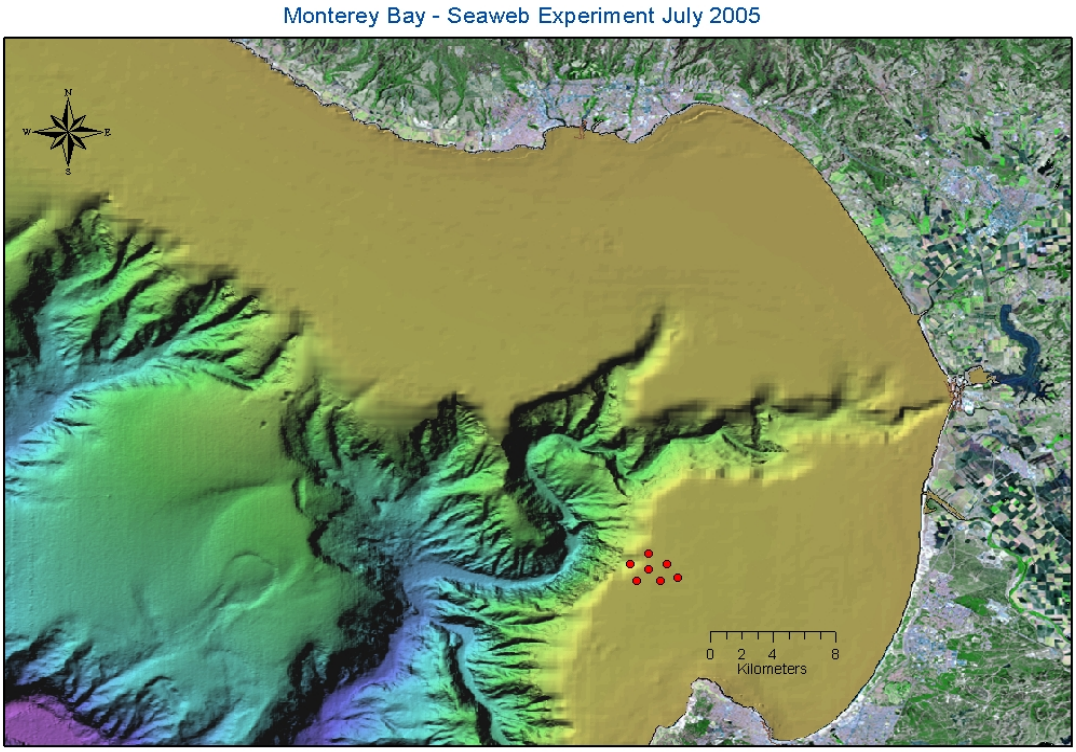

Figure 35. ArcGIS Map of Monterey Bay With Seaweb Node Positions

Prior to the experiment, a CTD cast was taken in the vicinity of the network. Using salinity, temperature and pressure measurements in the water column, the sound speed at all depths is calculated and is exhibited in Figure 36. This sound speed profile is then used to calculate paths of sound rays as they traveled through the water. Two

hundred ray paths are shown in Figure 37 at vertical angles ranging from -10^{o} to 10^{o} the horizontal axis. The source depth used in the calculation was 95 m, which is representative of a seafloor repeater node.

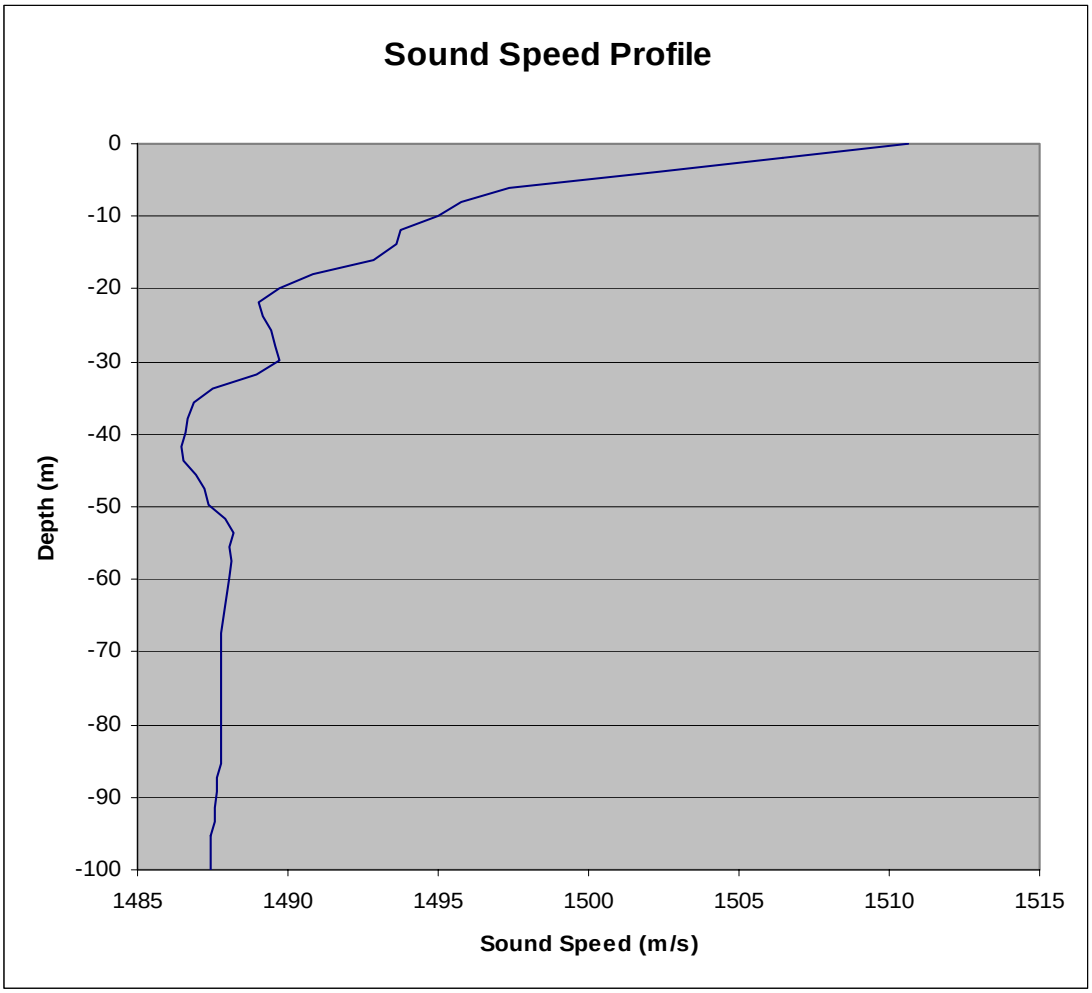

Figure 36. Sound Speed Profile

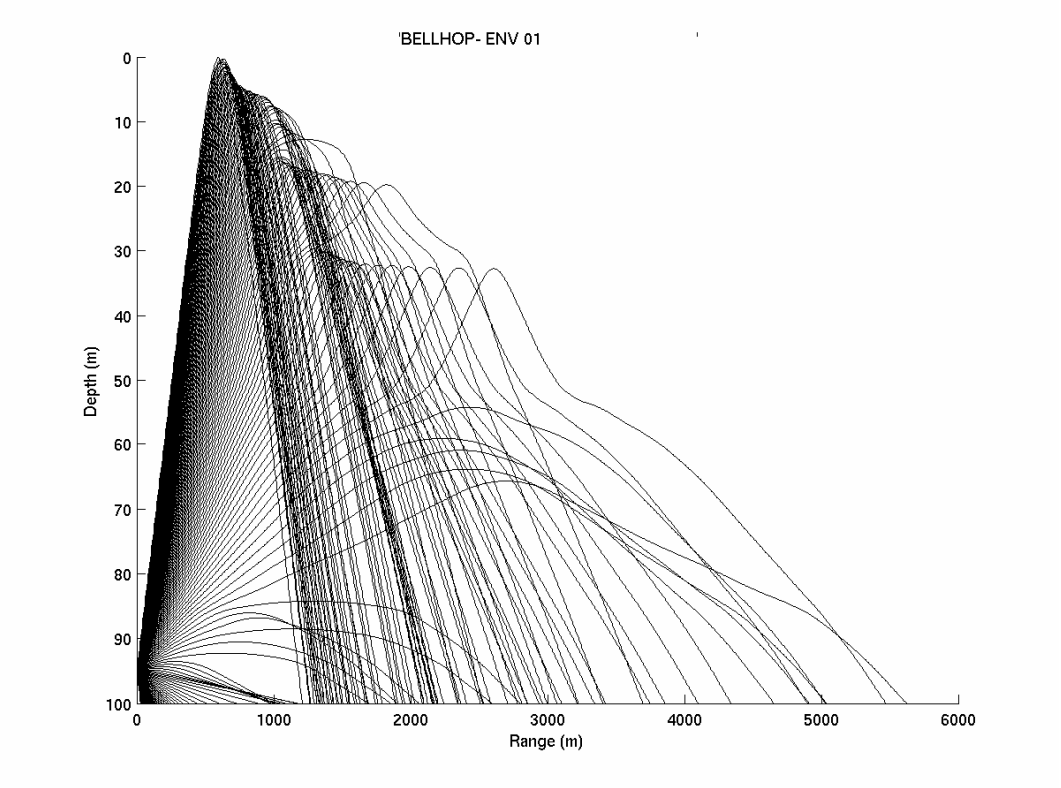

Figure 37. Ray Traces for a Source Depth of 95 m in the Vicinity of the Experiment

On July 20th, the Seaweb nodes were deployed at the locations specified in Table 1. The design was meant to be shaped like a pentagram with five outer nodes extending 1000 m from a central node. Since an Acoustic Doppler Current Profiler (ADCP) sensor with an attached acoustic modem was also in the vicinity, it was also used as a node in the network.

Node	Latitude (Decimal Degrees)	Longitude (Decimal Degrees)	Depth (m)
R10	36.70563	-121.96362	104
R11	36.71463	-121.96367	112
R12	36.70837	-121.95308	104
R13	36.6984	-121.95702	102
R14	36.69864	-121.96871	107
R15	36.70852	-121.97417	137
S21(ADCP)	36.70053	-121.94692	100

Table 1. Positions of Each of the Seven Nodes Used in Seaweb-Glider Experiment.

All node positions are converted to relative positions in meters referenced to the center node (Table 2). Referencing everything to a center node is an arbitrary choice for ease of presentation of data and graphs. In order to do the longitude (x position) conversion, the longitude difference is multiplied by 110972 m (the distance corresponding to one degree of longitude at 36^o latitude) and multiplied by the cosine of the average latitudes (35 and 36) [8].

$$\begin{aligned} \delta_{long,ab} &= long_a - long_b \\ \delta_{lat,ab} &= lat_a - lat_b \end{aligned} \tag{35}$$

$$x_{ab} = 110972 \cdot \delta_{long,ab} \cdot \cos\left(\frac{\delta_{lat,ab}}{2}\right) \tag{36}$$

Node #	Latitude Difference (m)	Longitude Difference (m)	Height Above Center (m)
R10	0.00	0.00	0
R11	998.75	-3.05	-8
R12	304.06	639.71	0
R13	-802.33	397.51	2
R14	-775.69	-306.62	-3
R15	320.71	-640.39	-33
S21(ADCP)	-565.96	1007.49	4

Table 2. Positions of Nodes Relative to Center Node.

I. EXPECTATIONS

In the May 2005 Experiment, ENS Hahn was able to track ARIES with a great deal of accuracy. As mentioned earlier, his algorithm used the weighting method but did not account for depth differences. It assumed that all nodes were always on the same x-y plane as ARIES. With the more accurate center-of-mass method and by accounting for depth corrections, the tracking of the Glider in the July Experiment should be an improvement, even with the large depth variation of all components.

C. DATA COLLECTED (GPS, DEAD RECKONING, RANGING)

During each day's testing, the Glider was deployed at around 500 m west of the center node. Tracks were designed to run a straight course while periodic broadcast ping data were taken. As the Glider ran a mission, it collected GPS data when at the surface and logged its DR position when underwater. These data points are spaced as little as a

second apart at many points along its track. The average time between broadcast pings is close to three minutes. All data are included in section C of the Appendix.

1. July 20

After deploying the nodes and racom buoy on the 20th, the Glider was launched at a relative x,y position of (-329.58, 219.54). The entire day's mission consisted of a 25-minute track and a 45-minute underwater track, punctuated by GPS fixes at the sea surface. The data taken are shown in Figure 38. For closer examination, the two tracks are individually plotted in Figures 39 and 40. The green lines represent best fit lines for the Seaweb ranging positions. A solid red line connects GPS fixes and black arrows denote the general direction of the Glider.

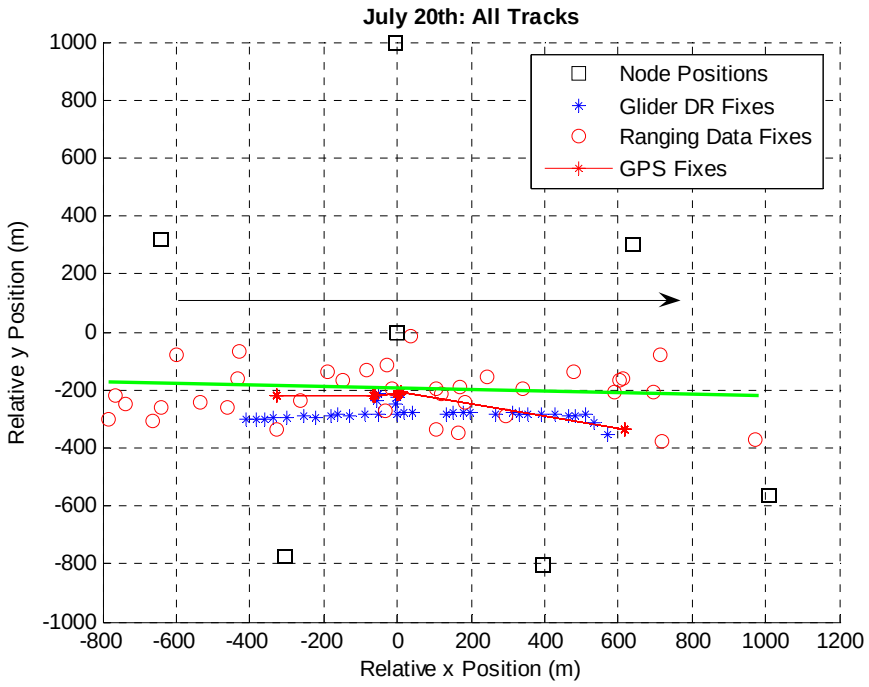

Figure 38. July 20 Glider Track.

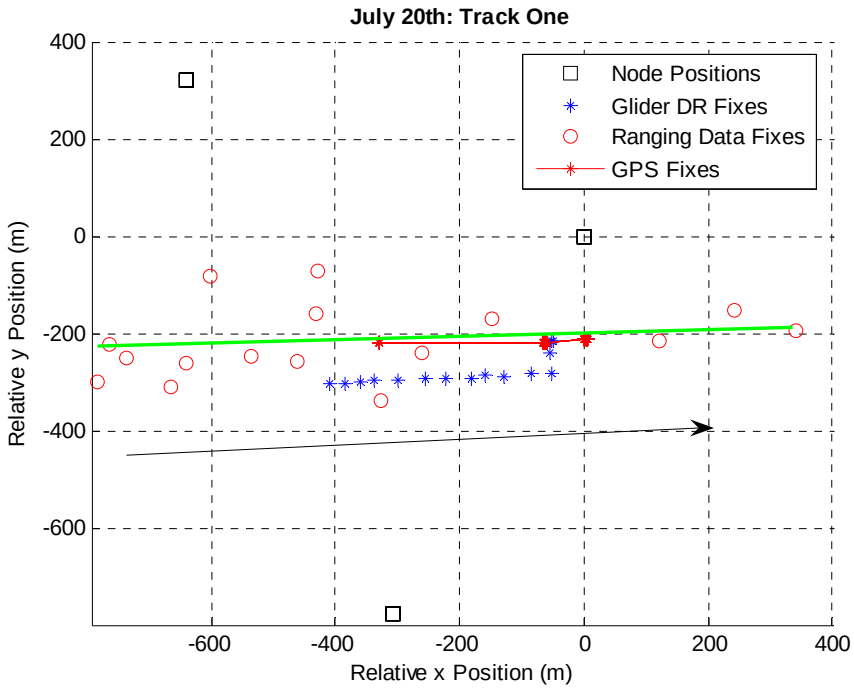

Figure 39. July 20: Track One

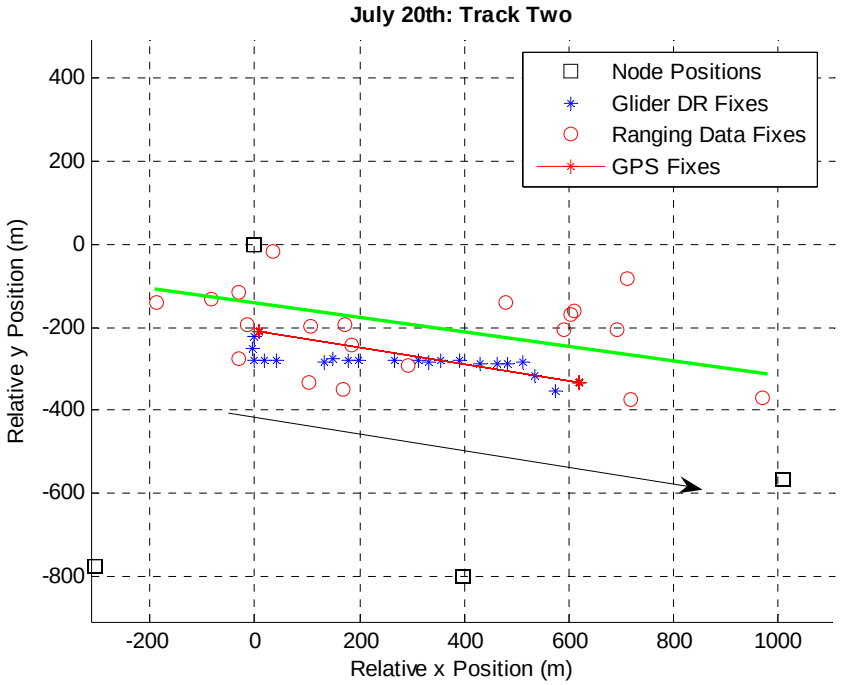

Figure 40. July 20: Track Two

It is evident from the Track 2 data for the 20th that the positioning algorithm has difficulty in accurately tracking the Glider. While the best fit line appears to be close to

the line between GPS points, there are large errors in the individual fixes. By looking at the range circles that result from the data, some understanding of these errors can be gained (Figure 41).

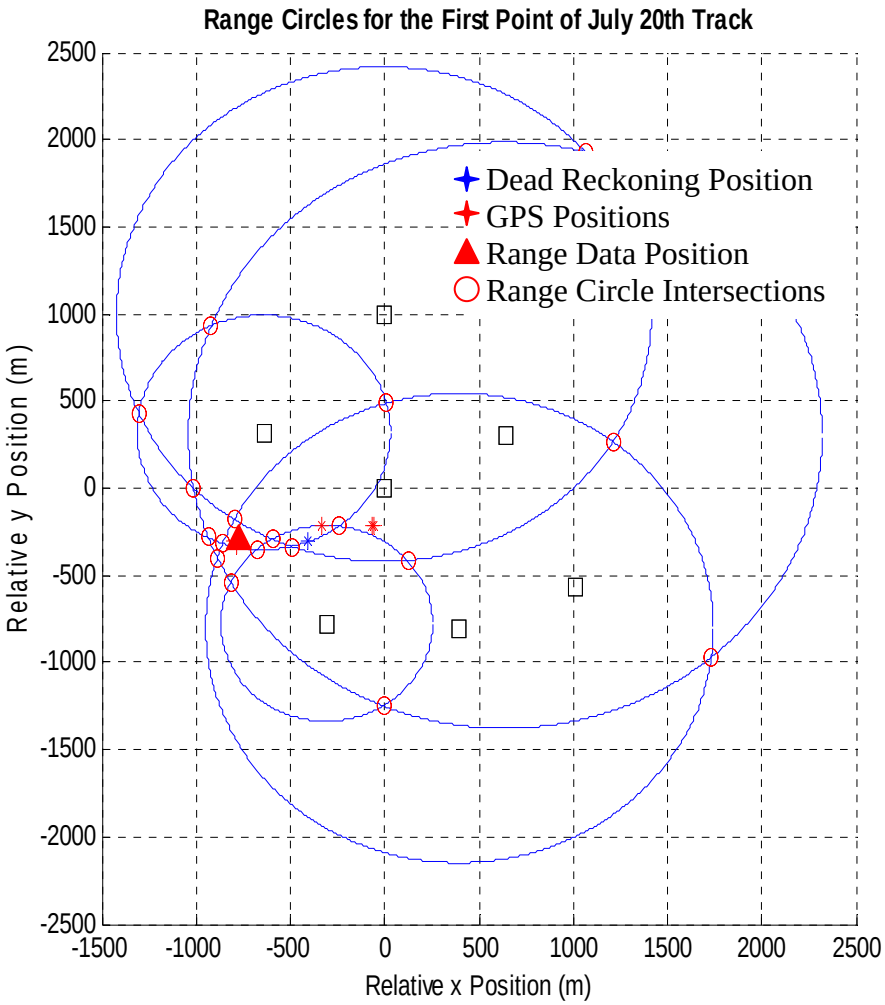

Figure 41. Range Circles for a Ping Time on July 20th

Figure 41 clearly shows that the range circles do not form a cluster in proximity to the Glider position. This leads one to believe that there were problems in the range data. Using ENS Hahn's algorithm to compute the position with the same data also led to similar errors, concluding that there are errors in the ranging data or other systematic errors.

One explanation of this ranging error is the fact that, in the July conditions, a sound ray refracts more because of the larger gradient in sound speed. As shown in Figure 36, the sound speed varied in the water column by up to 24.12 m/s. Using the 1500 m/s assumption in this experiment, the calculated ranges would be skewed. For a source and receiver both at the depth of the maximum sound speed at a range of 1000 m, the true travel time would be 1000 m divided by 1510.6 m/s (the greatest sound speed in the water column), which equals 0.662 s. This time multiplied by the 1500 m/s assumption gives a range of 992.98 m. At the depth of minimum sound speed (1486.48 m/s), the range would be 1009.1 m. These differences are small in themselves, but additional complications occur when the source and receiver are at different depths. In Figure 37, the ray trace diagram reveals that for certain receiver depths and ranges, the sound waves travel much farther than the straight-line distance between the two.

2. July 21

Since the major set-up of the experiment was completed on the 20th, the 21st served as the main day for data collection. Data were collected for four major tracks that were all longer than those from the 20th. The track durations are one hour, six minutes; one hour, five minutes; 43 minutes; and one hour, 13 minutes, respectively. The tracks are shown in Figures 42-45. These data are all analyzed using the center-of-mass method.

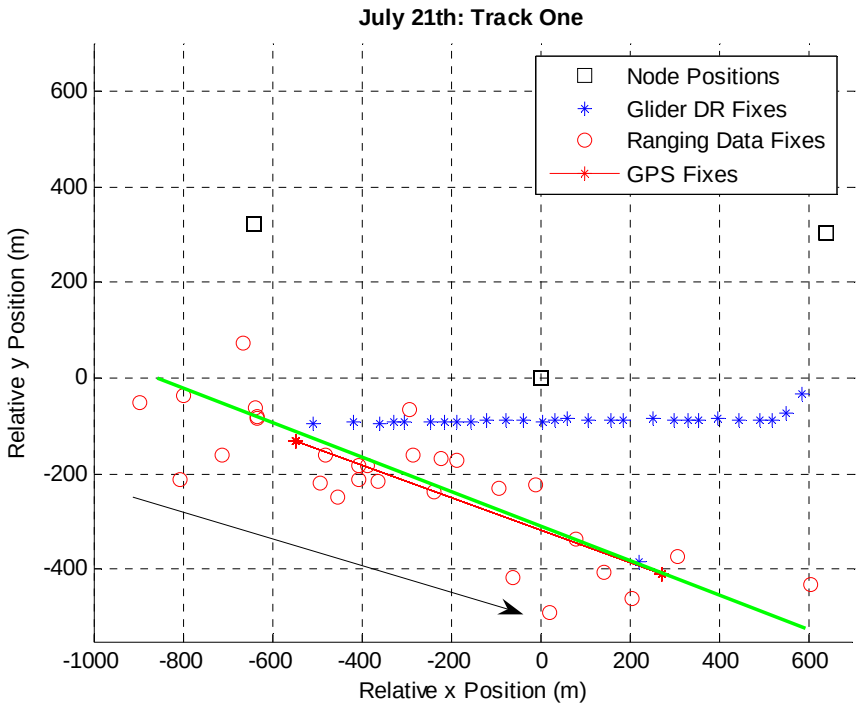

Figure 42. July 21: Track One

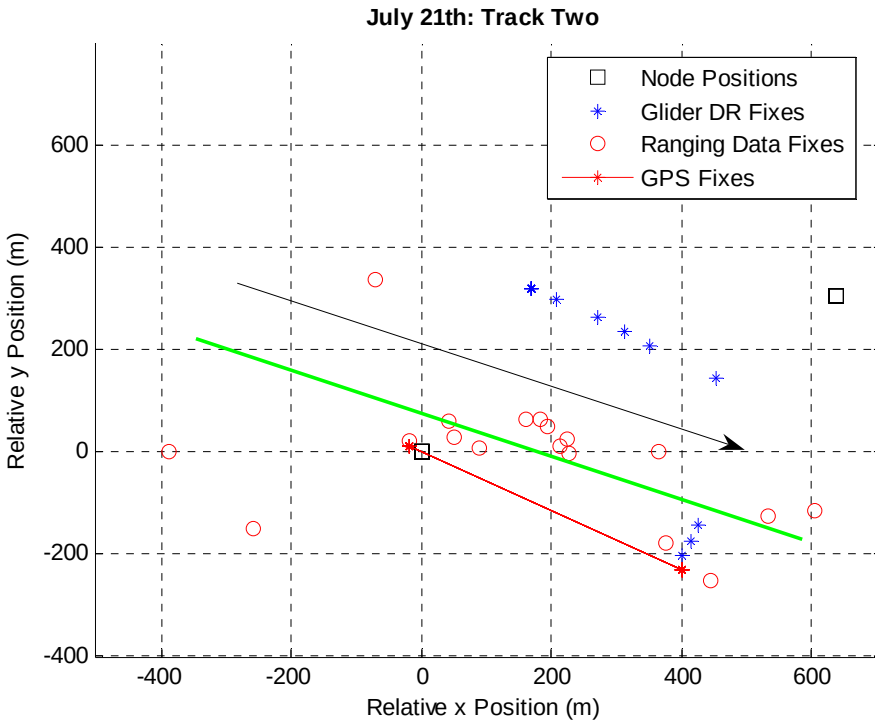

Figure 43. July 21: Track Two

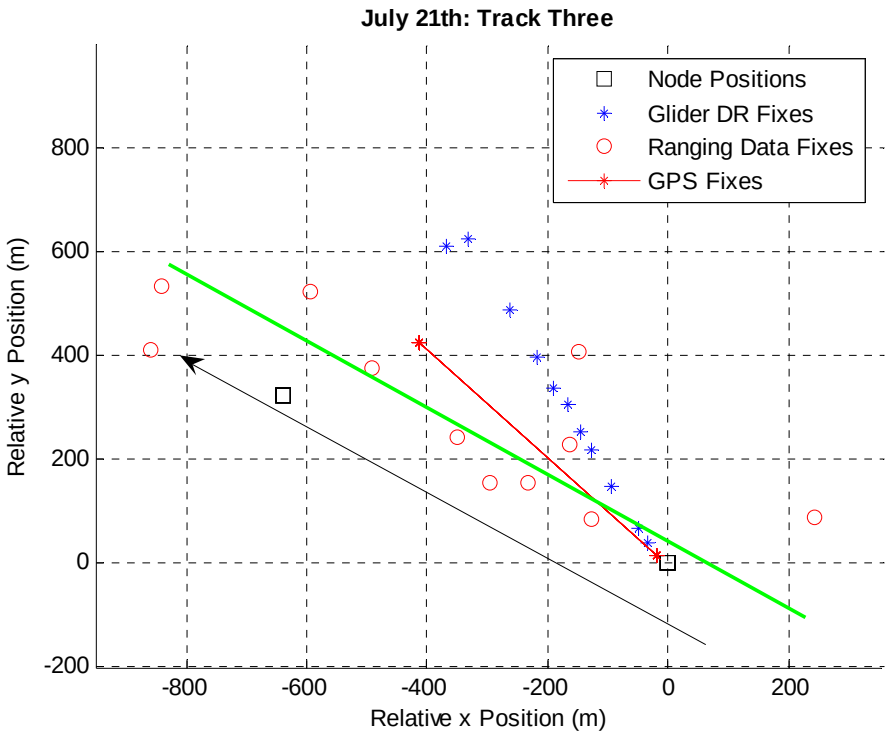

Figure 44. July 21: Track Three

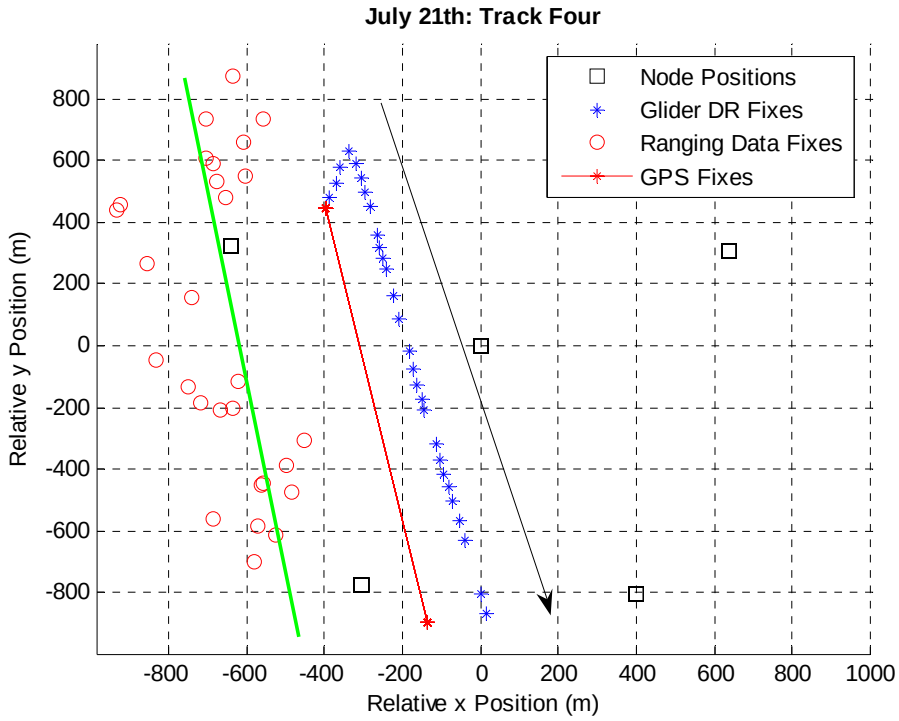

Figure 45. July 21: Track Four

As seen by the data for the 21st, the best fit lines of the ranging data appear to be quite close to the GPS data, but there are large errors in the individual fixes. Tracks two and four show large disconnects between the first DR position and the previous GPS fix because the mission was started some time after that previous GPS fix. Water currents, then, led to the drift of the Glider away from the last GPS fix. Track four particularly exhibits this drift.

3. July 22

The final day of testing resulted in only one track which lasted for one hour and 14 minutes (Figure 46). Again, the same methods of Glider positioning were used.

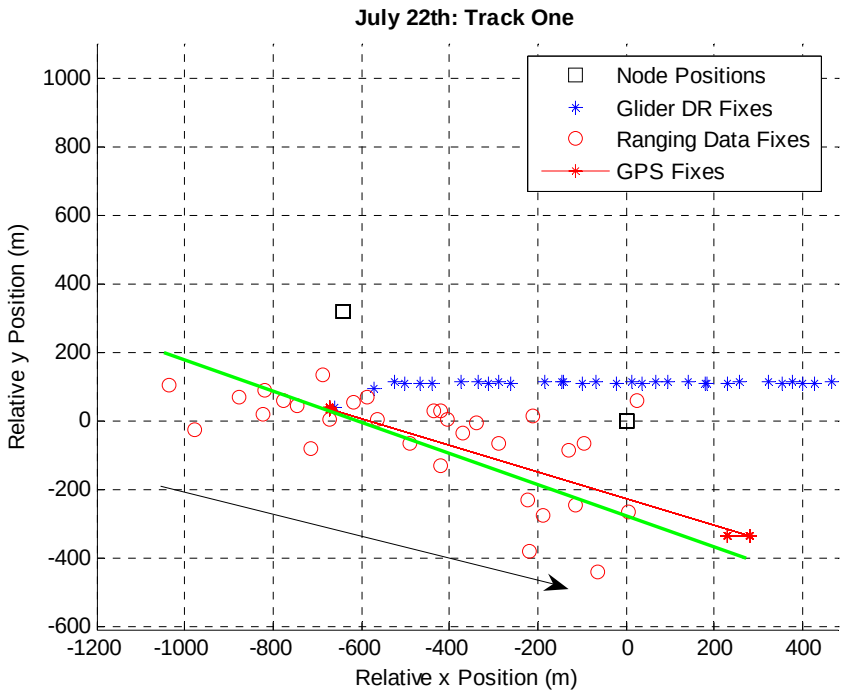

Figure 46. July 22: Track One

THIS PAGE INTENTIONALLY LEFT BLANK

VII. CONCLUSIONS AND IMPROVEMENTS

A. RESULTS

The revised center-of-mass algorithm proved to be a more effective means of positioning the Glider over the weighting method used by ENS Hahn. This was shown in simulation one and further justified in simulation two. With real data, however, positioning was difficult. The error is believed to be due to the method of calculating the range for each ping, as well as environmental factors.

B. POSSIBLE SOURCES OF ERROR

Many sources of error existed in this experiment. The first sources result from the determination of the seafloor node positions. As the *Cypress Sea* approached the deployment point, a handheld GPS sensor was used to give the position directly above each node's release. Along with the errors present in such a GPS receiver, the node may have drifted some as it sank to the seafloor because of water currents. Depth measurement also contained some error because it was measured by reading off the fathometer onboard the *Cypress Sea*.

Several of the tracks seemed to have best fit lines with similar slopes to the GPS line. It appears in several of the cases that the slope of the best fit line to the ranging data correlates well with the GPS line. This leads to the belief that the nodes may have shifted its true position as it sank in the water column upon deployment. The deeper water in this experiment could lead to the shift of the node away from the GPS fix by several meters.

Another source of error results from the movement of the Benthos modem around the sandbag due to water currents. This error would be very small, though, since the modem rises above the sandbag by only three meters. A very strong current, then, would only change the modem's true position by roughly two meters.

The effects of multipath sound rays are also contributing to error. If an omni-directional sound signal is sent to the Glider, some of those rays will reflect off of the seafloor or the sea surface before reaching the Glider. If two reflected rays reach the Glider at the same time, then the source level of that signal will be high and may cancel

out the direct path signal which may not have been as strong. In addition, the matched filter detection may produce multiple peaks associated with multipath that may be stronger than the direct-path peak.

Since the nodes all had a random dwell of up to a few minutes, some ranging error would be present because of the Glider's movement over that time. While this wouldn't play a large role with the Slocum Glider (which travels at close to 0.5 m/s), a faster UUV would encounter much higher errors. Even at 0.5 m/s, though, a one minute dwell at a node could correspond to a 30 m difference. This would then affect the range that is calculated from the total travel time.

Lastly, the largest errors are due to the fact that the sound speed varied significantly in 100m of water. This variation leads to changes in the travel times of the sound signals, which can greatly affect the ranges that are calculated.

C. FURTHER WORK AND IMPROVEMENTS

1. Grid Self-Positioning

One improvement that would limit some error would be to have the nodes position themselves based on their ranges to each other. This would mitigate some of the error due to any currents that deflect the node as it is sinks to the bottom. While no single node would have an exact location, all nodes could be positioned relative to each other which could lead to better accuracy.

2. Physics-based Ranging

An algorithm that incorporates information about the sound speed profile in the water column would greatly improve Glider positioning. By accounting for the curve and speed of the ray path as it travels from source to receiver, the true distance can be calculated much more accurately.

3. Determining Position When Depth is Unknown

A third improvement to the current algorithm involves tracking an undersea vehicle without a known depth. This would require a much more robust algorithm, but is absolutely possible. This would then allow the Seaweb system to track a different type of UUV which does not have a depth sensor onboard.

4. Automation of Data Collection and Integration of Algorithm onto the Glider

Currently, a major problem with the method of data collection and Glider positioning is that it is not real time. After a broadcast ping has traveled to each node and back to the Glider, it is sent to the racom buoy and then to the command center. The data must then be manually entered into a file and loaded into the MATLAB program to calculate the position. Especially for an undersea vehicle that moves quickly through the water, this delay is far too large.

One improvement is to have the data coming from the racom buoy automatically entered into the MATLAB program for near-real-time tracking. With powerful enough computing equipment, this could occur almost instantaneously. Eventually, a goal of this work is to have the Glider position itself based on the broadcast pings. This would give it a more accurate and near real-time position to allow it to stay below the water's surface for extended periods of time. This implementation onto the Glider could lead to the eventual goal of having a school of Gliders operating collaboratively. Some of these Gliders could be at the surface, receiving constant GPS positions while others are underwater, conducting whichever mission is required of them. Sending out pings to each other could then lead to positioning without the need for nodes on the seafloor.

THIS PAGE INTENTIONALLY LEFT BLANK

LIST OF REFERENCES

1. Kriewaldt, H., *Communications Performance of an Undersea Acoustic Wide-Area Network,* Naval Postgraduate School Master's Thesis, (2005).

2. Kalscheuer, J., *A Selective Automatic Repeat Request Protocol for Undersea Acoustic Links,* Naval Postgraduate School Master's Thesis, (2004).

3. Webb, D.C., Simonetti, P.J., and Jones, C.P. SLOCUM, An Underwater Glider Propelled by Environmental Energy, IEEE Journal of Oceanic Engineering, Vol. 26, No. 4, October 2001.

4. Webb Research Corporation. Slocum Battery Glider: Operations Manual SSC-SD Ver 1.3. 8 April 2005.

5. Mailey, Chris. Monterey Bay Glider Operation Notes. SPAWAR Systems Center San Diego. 2005.

6. Hahn, M., *Undersea Navigation Via a Distributed Acoustic Communications Network,* Naval Postgraduate School Master's Thesis, (2005).

7. Rice, J. *Hydrophone Localization in a Sonobuoy Array*, University of California San Diego Master's Thesis, (1990).

8. National Geospatial-Intelligence Agency. Length of a Degree of Latitude and Longitude. 11 Sep 2005. http://pollux.nss.nima.mil/calc/degree.html.

THIS PAGE INTENTIONALLY LEFT BLANK

APPENDICES

A. MATLAB CODE FOR SIMULATIONS AND TRACKING WITH BOTH ALGORITHMS

1. Main Program

```
%This program was used to run simulation one with the center of mass method
%It also contains all parts to run simulation two and track the glider with
%real data

close all %closes all open figure windows
clear all %clears all variables, functions, etc from memory
clc       %clears command window

node_pos=xlsread('program_stationary_nodes'); %node_pos will read from an
   %excel file to take the positions of the nodes that were used in the
   %experiment

%-------------------------------------------------------------------------
%glider_pos=xlsread('simulation2_inner'); %used for the simulation of the
                                          %inner track
%glider_pos=xlsread('simulation2_outer'); %used for the simulation of the
                                          %outer track

%glider_pos=xlsread('program_jul20_glider_ins_pos'); %used to read in the
   %dead reckoning positioning data from the Glider.
%glider_pos=xlsread('program_jul21_glider_ins_pos');
%glider_pos=xlsread('program_jul22_glider_ins_pos');
%-------------------------------------------------------------------------

%-------------------------------------------------------------------------
%gps=xlsread('program_jul20_gps_fix); %Imports excel files with the gps
%gps=xlsread('program_jul21_gps_fix); %data for each day
%gps=xlsread('program_jul22_gps_fix);
%-------------------------------------------------------------------------

% This loop will determine the node to node ranges (internode_ranges(i,j)),
% which are straight line distances, as well as those ranges translated to
% the xy plane. This length, internode_ranges_xy (or rij in diagrams), will
% be less than the straight line distance unless the two nodes are at the
% same depth.

for(i=1:1:size(node_pos,1));
   for(j=1:1:size(node_pos,1));
```

```
      if(i~=j);
         x_diff(i,j)=node_pos(i,1)-node_pos(j,1);
         y_diff(i,j)=node_pos(i,2)-node_pos(j,2);
         z_diff=node_pos(i,3)-node_pos(j,3);
         internode_ranges(i,j)=sqrt(x_diff(i,j)^2+y_diff(i,j)^2+...
            z_diff^2);
         internode_ranges_xy(i,j)=sqrt((internode_ranges(i,j)^2-...
            z_diff^2));
      end
   end
end

G=input...
   ('Enter the number of times the glider position should be simulated');

%For simulation 2, G=1:1:size(glider_pos,1).
for (i=1:1:G); %make a list of positions equal to G for the simulation
    glider_pos(i,1)=(.5-rand(1))*2000;
    glider_pos(i,2)=(.5-rand(1))*2000;
    glider_pos(i,3)=(rand(1)*100);
end

% To find the ranges that would be present between the glider and each node
% a matrix is created to determine the distances with some random error, as
% was seen in the experiment. ping_ranges(g,k) looks at the glider position
% for each (g) and gives the range to each node for that step in the loop
% (g=1:1:G). An error of up to +/- 10m is used and added to the ranges.
% ping_ranges_xy(1,k) takes the range when transformed down to the xy plane
% as described in Chapter IV.

for (g=1:1:G);
   clear xfinal2 yfinal2 xgood ygood yoga xoga yogb xogb xogab yogab %This
      %clears all variables that may change in length for different
      %values of g.

   %-------------------------------------------------------------------
   %ping_ranges=xlsread('program_jul20_ping_ranges'); %These commands read
      %in files which contain the ping ranges for each day's data
   %ping_ranges=xlsread('program_jul21_ping_ranges');
   %ping_ranges=xlsread('program_jul22_ping_ranges');
   %-------------------------------------------------------------------

   for (k=1:1:size(node_pos,1));
      ping_ranges(g)=sqrt((node_pos(k,1)-glider_pos(g,1))^2+...
         (node_pos(k,2)-glider_pos(g,2))^2+...
         (node_pos(k,3)-glider_pos(g,3))^2);
```

```
   %ping_error(g)=0; %No ping error was used for figures 27 and 28
   ping_error(g)=20*(.5-rand(1)); %Used for a +/- 10m range error
   ping_ranges(g)=ping_ranges(g)+ping_error(g);
   ping_ranges_xy(g,k)=sqrt((ping_ranges(g))^2-(node_pos(k,3)-...
      glider_pos(g,3))^2);
end

% Now the ranges between each node as well as the ranges from each node
% to the glider have been determined at every step from 1:1:G. These
% have also all been translated onto the xy plane. The next step is to
% find which triangles form real solutions. While all nodes would have
% ranges in this simulation, not all ranges were found at every time
% step in the experiment. Solution are only going to be present for
% range circles that touch, though. The situation described in Chapter
% IV, section E, part 1 will not be taken into account since it has no
% real affect on the final solution

   for (i=1:1:size(node_pos,1));
      r1=ping_ranges_xy(g,i);
      for (j=1:1:size(node_pos,1));
         if(i~=j);
            r2=internode_ranges_xy(i,j); %These give the three
            r3=ping_ranges_xy(g,j);      %sides of the triangle
            theta(i,j)=law_of_cosines(r1,r2,r3); %theta will give
            %the angle between the two nodes and node i to the
            %glider(Chapter IV)
            if(isreal(theta(i,j))==1);
               theta_good(i,j)=theta(i,j);
            else
               theta_good(i,j)=NaN;
            end
         end
      end
   end

% Each good pair of nodes (that also have ping ranges) will give an xy
% solution. Because of errors and delay times, these positions will not
% be the same as for all other pairs' solutions. Factoring all of them
% together will lead to a real, approximate solution. Values for
% theta_good for all solutions at each ping time have now been
% calculated. The following will calculate phi and then gamma for each
% solution.

count=0;
for(i=1:1:size(node_pos,1)); %i from 1 to 7
   for(j=i+1:1:size(node_pos,1)); %Only compare the 1st node to all
```

```
%others and then the second to nodes 3-7, and so on
if isnan(theta_good(i,j))==0 & (i~=j); %if theta_good is not
   %NaN, then look at that i,j combination
   count=count+1;
   if (x_diff(i,j)==0); %if both nodes happen to lay directly
            %n-s of each other (not necessary for this
            %experiment, but may be needed for a future
            %experiment, and...
      if (node_pos(i,2)<node_pos(j,2)); %the y
         %value of node i is less than the y value of
         %node j (figure 17)...
         phi_prime=pi/2; %then phi (the angle between the x
            %axis and the line between the two nodes with
            %node i as the origin) is pi/2) and...
         phi(i,j)=phi_prime;
      else phi_prime=-pi/2; %If the y value of node i is
         %larger, then phi is -pi/2
          phi(i,j)=phi_prime;
      end
   else phi_prime=atan(abs(y_diff(i,j))/abs(x_diff(i,j))); %If
      % the x difference is NOT 0 between the two nodes,
      % and...
      if ((node_pos(i,1)<node_pos(j,1))&...
        (node_pos(i,2)<=node_pos(j,2)));
         phi(i,j)=phi_prime; %In first quadrant
      elseif((node_pos(i,1)>node_pos(j,1))...
        &(node_pos(i,2)<=node_pos(j,2)));
         phi(i,j)=pi-phi_prime; %In second quadrant
      elseif((node_pos(i,1)>node_pos(j,1))&...
        (node_pos(i,2)>=node_pos(j,2)));
         phi(i,j)=pi+phi_prime; %In third quadrant
      elseif((node_pos(i,1)<node_pos(j,1))&...
        (node_pos(i,2)>=node_pos(j,2)));
         phi(i,j)=-phi_prime; %In fourth quadrant
      end
   end

   gamma_a(i,j)=phi(i,j)+theta_good(i,j); %Each set of nodes
      %will give two values of gamma corresponding to the two
      %solutions
   gamma_b(i,j)=phi(i,j)-theta_good(i,j);

   % The following part will be used for finding the solutions
   % using the center of mass method. xoga is the x value from
   % the center node to the glider for solution a. Since
   % either solution a or b will be good, only one will be
```

```
            % kept

            xoga(count)=node_pos(i,1)+ping_ranges_xy(g,i)*...
               cos(gamma_a(i,j)); %This is the first x value of the
                  %solution for every i,j combination
            xogb(count)=node_pos(i,1)+ping_ranges_xy(g,i)*...
               cos(gamma_b(i,j)); %This is the second x value of the
                  %solution for node i
            yoga(count)=node_pos(i,2)+ping_ranges_xy(g,i)*...
               sin(gamma_a(i,j));
            yogb(count)=node_pos(i,2)+ping_ranges_xy(g,i)*...
               sin(gamma_b(i,j));
         end
      end
   end

% Calculate center of mass for all the points

xogab=[xoga xogb]; %Combines all xoga and xogb into one vector
yogab=[yoga yogb];

cmx=nanmean(xogab); %nanmean takes the mean of all numbers and
cmy=nanmean(yogab); %doesn't account for anything that is NaN

% Now, throw out the point that is farther away from the center of mass
% between the two [(xoga,yoga) or (xogb,yogb)]

count=0; %A counter is started that will only increase by 1 every
   %time a certain condition is met
for c = 1:count;
   cmadiff(c)= sqrt((cmx - xoga(c))^2 + (cmy - yoga(c))^2);
      %Calculates the distance between the center of mass and
      %solution a
   cmbdiff(c)= sqrt((cmx - xogb(c))^2 + (cmy - yogb(c))^2);
   if cmadiff(c)==NaN    %For an xoga,yoga pair that is not a number
      %(happens when the range errors shrink the ranges so that theta
      %is imaginary), make the distance to the center of mass very
      %large
      cmadiff(c)=10000;
      break
   end
   if cmbdiff(c)==NaN;
      cmbdiff(c)=10000;
      break
   end
   if cmadiff(c) <= cmbdiff(c); %Only use the point that is closer of
```

```
        %the two
      count=count+1;
      xgood(count) = xoga(c);
      ygood(count) = yoga(c);
   else
      count=count+1;
      xgood(count) = xogb(c);
      ygood(count) = yogb(c);
   end
end

cmx2=nanmean(xgood); %Take the new center of mass of the good points
cmy2=nanmean(ygood);

good_count=0;
for c = 1:count;
   cmadiff(c)= sqrt((cmx2 - xoga(c))^2 + (cmy2 - yoga(c))^2);
   cmbdiff(c)= sqrt((cmx2 - xogb(c))^2 + (cmy2 - yogb(c))^2);
    if cmadiff(c)==NaN
      cmadiff(c)=10000;
      continue
   end
   if cmbdiff(c)==NaN;
      cmbdiff(c)=10000;
      continue
   end
   if cmadiff(c) <= cmbdiff(c);
      good_count=good_count + 1;
      xgood(good_count) = xoga(c);
      ygood(good_count) = yoga(c);
   else
      good_count=good_count + 1;
      xgood(good_count) = xogb(c);
      ygood(good_count) = yogb(c);
   end
end

% Now, take another center of mass to calculate the final position
xfinal2=nanmean(xgood);
yfinal2=nanmean(ygood);

sdxfinal=nanstd(xgood);
sdyfinal=nanstd(ygood);

%-----------------------------------------------------------------------
%The following part was used to run simulation one with the weighting
```

```
%method

%W=zeros(size(xogab,1),1);
%for(i=1:1:size(xogab,1));
   %for(j=i+1:1:size(xogab,1));
      %factor=100;
      %delta_x(i,j)=xogab(i)-xogab(j); %Find the difference in x
         %position between every solution and every other solution
      %delta_y(i,j)=yogab(i)-yogab(j);
      %dxy=(delta_x(i,j))^2+(delta_y(i,j))^2;
      %if dxy>=1;        %For two solutions that are far from
         %W(i,j)=(1/dxy) %each other, this is the weight value
      %else              %If they are very close, they get a weight
         %W(i,j)=factor; %of 100
      %end
   %end
%end
%Wsum=sum(nansum(W)); %Take the sum of all of the weights. Since W
                     %will be a 2 dimensional matrix, sum up the
                     %columns first, and then sum those up

%Each xogab,yogab solution now has a weight. Taking each solutions
%weight and dividing by the total weight will give a percentage of
%total weight for that solution. Multiplying that percentage by its x
%and y position will contribute to the final solution. The higher the
%weight percentage, the higher the contribution.

%for i=1:1:length(xogab);
   %for j=1:1:length(xogab);
      %x_fin(i,j)=W(i,j)/Wsum*xogab(i);
      %y_fin(i,j)=W(i,j)/Wsum*yogab(i);
%end
%end

%xfinal2=sum(nansum(x_fin));
%yfinal2=sum(nansum(y_fin));
%-------------------------------------------------------------------

hold on

%-------------------------------------------------------------------
%plot(glider_pos(g,1),glider_pos(g,2),'b*') %These were all used to
   %make graphs for real data and for simulation two
%plot(node_pos(:,1),node_pos(:,2),'ks')
%plot(xogab,yogab,'ro','MarkerSize',5)
%plot(xgood,ygood,'ro','MarkerSize',10)
```

```
    %plot(xfinal2, yfinal2,'+r','MarkerSize',10)
    %plot(gps(b,1),gps(b,2),'r*')
    %-------------------------------------------------------------------

    error(g)=sqrt((xfinal2-glider_pos(g,1))^2+(yfinal2-...
       glider_pos(g,2))^2); %Used in simulations

end %This closes the primary loop

ave_error=mean(error)
sd_error=std(error)
max_error=max(error)

figure(2)
hist(error,20)
sorted_error=sort(error); %Sorts all error values
percent50_error=sorted_error(.5*G)  %These give the percentiles of error
percent75_error=sorted_error(.75*G) %for the simulations
percent90_error=sorted_error(.9*G)
percent95_error=sorted_error(.95*G)
percent99_error=sorted_error(.99*G)
```

2. Law of Cosines

```
%This function will calculate the angle across from one side of a triangle
%(side 3)given the lengths of all three sides

 function law_of_cosines(A,B,C);

 angle=acos((C^2-A^2-B^2)/(-2*A*B))
```

3. Drawing a Circle

```
function draw_circle2(xo,yo,r) %r is the radius with center at xo,yo

%define the circle equations
x=[xo-r:0.1:xo+r]; %Plot the circumference starting out at range r from the
    %center. This starts at xo - r (left side of the circle) with steps in
    %x of .1 (which can be larger to improve speed of the program)
y_top=yo+sqrt(r^2-(x-xo).^2); %This plots the y values for the top half of
    %the circle. Gives a y value for each x
y_bottom=yo-sqrt(r^2-(x-xo).^2); %Same for bottom

%plot the equations defined above, over the appropriate intervals
hold on
grid
plot(x,y_top,'b-')    %Plot the top of the circle as a blue line
plot(x,y_bottom,'b-') %Same for bottom
```

```
plot(xo,yo,'ks')      %Plot the node position as a black circle of size 12,
                      %filled in with black
xlabel('Relative x position (m)')
ylabel('Relative y position (m)')
title('Node positions and Range Circles')
```

B. OTHER USEFUL CODE FROM THIS WORK

1. MATLAB Code For Figure 15 (Range Estimation Error)

```
%This matlab program was used to plot figure 20 (Range Estimation Error)

x=1:1:1000; %Vary the horizontal distance from 1m to 1000m
z=100;      %Fix the water depth at 100m

r=sqrt(x.^2+z^2);      %r is then the hypotenuse of the triangle
error=(1-(x./r))*100; %error is the difference between r and x

plot(x,error); %plot x on the x axis and error on the y axis
title('Errors In 2D Range Estimates for a 3D System (Depth = 100m)')
xlabel('Horizontal Range From Node to Glider (m)');
ylabel('Error Present for Z = 100m');
annotation('textbox','Position',[.55,.45,.3,.15],'String',{'1% Error ~...
   707m Horizontal Range','5% Error ~ 320m Horizontal Range','10% Error ~
   230m Horizontal Range'}); %This makes a text box with opposite corners at
   (.35,.45) and (.3, .15), which reads the errors off at the three different errors.
```

C. DATA COLLECTION

1. July 20th (GPS Fix Times are in Red with Unavailable Data in Blue)

	Node Number							Relative Glider INS Position (m)			Distance from Center
Time	R10	R11	R12	R13	R14	R15	R21	Latitude	Longitude	Height	
11:41:23								219.54	-329.58	101.00	408.68
12:04:00		1421.7	1683	1348.9	567.9	681.9		301.02	-408.81	83.18	514.45
12:06:05	649.8	1408.5	1636.8		564.9	699.9	2157.9	303.37	-384.01	69.60	494.30
12:08:16	612.9	1376.7	1599.3	1259.7	572.8	723.1	2119.9	299.14	-359.19	52.18	470.35
12:10:05		1365.1	1569.4		567	731.1		296.72	-337.64	36.88	451.00
12:12:16	557.7	1344.3		1221.6	579.4	740.7	2060.2	296.85	-300.67	42.92	424.69
12:14:13	514.2	1331.5		1173.9	603.1	785.8	2011.8	291.58	-255.17	72.09	394.12
12:16:04	468.9	1306.8		1126		809.4	1977.7	292.95	-223.64	78.00	376.73
12:19:59	412	1285.2		1077.1	648.1	849.7	1894	292.23	-181.63	49.68	347.65
12:21:52	375	1277.8		1047.6	661.2	891.9		285.88	-159.54	34.78	329.22
12:23:36			1326	1033.9			1841.5	287.29	-130.17	40.67	318.02
12:25:32	320.7	1252.5	1292.5	1002.1	713.4	925.5		282.03	-85.73	69.91	302.95
12:27:20		1236.4	1241.2	962.5		959.4		282.53	-51.14	86.66	299.91
12:29:06	264.3	1246.2			774			237.62	-54.67	101.00	263.92
12:29:28								218.24	-65.92	101.00	249.35

12:29:33								217.69	-64.91	101.00	248.60
12:29:38								218.06	-64.00	101.00	248.69
12:29:45								218.06	-63.40	101.00	248.54
12:29:49								217.69	-62.49	101.00	247.98
12:29:54								217.51	-61.28	101.00	247.52
12:29:59								217.14	-60.47	101.00	246.99
12:30:54	248.2	1221.9			799.6		1702.2	216.29	-50.69	101.00	244.03
12:34:24	230.5	1248.3			840.4			216.27	-50.51	101.00	243.98
12:35:35								211.96	-0.71	101.00	234.79
12:35:46								211.59	3.12	101.00	234.48
12:35:51								211.40	4.03	101.00	234.32
12:35:56								211.40	5.24	101.00	234.35
12:36:00								211.03	6.25	101.00	234.04
12:36:04		1245.9				1116.7		210.54	6.99	100.87	233.56
12:36:12								209.55	8.47	101.00	232.78
12:37:52	228.7		1057.9	836.5		1115.1		222.61	-1.63	91.39	240.64
12:39:47	242.2	1229.5	1069	821.7	1103.8	1124.5	1563.4	248.95	-4.49	78.72	261.14
12:41:53	268.3		1076.5	794.5	849			280.72	-2.32	62.82	287.68
12:43:49	286.2	1279.6	1077.3	769.9	848.4		1523.8	278.67	19.48	46.58	283.21
12:45:41	285.1	1282.3	1033.2	742.8	873.6			278.20	41.34	30.54	282.90
12:51:21	362.7		930.9	662.2	986.8		1358.5	283.40	131.31	74.47	321.10
12:53:14	382.9	1303.5	910.9	639.1	1013.5			277.11	150.26	60.13	320.91
12:55:49	407.8	1317.9	874.5	740.1			1281.9	279.06	177.47	40.68	333.21
12:57:39	430			610.8	1079.5			280.30	197.33	32.59	344.34
13:01:22	507.9	1337.7	784	586.9			1171	281.13	267.58	84.01	397.10
13:04:39	569.8	1368.4	743.1	559.8			1102.5	279.13	312.77	61.70	423.73
13:06:29		1402.8	711.7	553.3	1249			283.88	333.59	45.12	440.34
13:08:15		1391.7		551.1	1275.4		1130.4	281.02	354.30	29.74	453.20
13:10:36	647.7	1404.9	671.5	566.1	1309	1650.9	1004.2	281.28	390.69	56.18	484.68
13:12:26		1430.2	649.6	567.7			955.8	286.17	429.21	83.11	522.52
13:14:23	753.6	1453	630.1	568.9	1405.9		902.5	286.96	462.86	71.30	549.25
13:16:17		1472.8	616.6	574.9	1444.5		868.3	286.89	483.82	55.17	565.18
13:18:41			765	584.5	1474.9			285.14	510.92	35.94	586.20
13:20:34	857.1		590.8	603.7	1508.2		805.6	315.62	535.29	58.91	624.20
13:22:40		1560.7	611.7	601	1551.6		750.4	354.49	572.58	92.91	679.82
13:24:09								334.03	618.66	101.00	710.29
13:25:34			635.1	612.6			670.2				
13:28:02		1669.9	639.4								
13:30:08		1692.9	645.9	634.8	1678		611.5				

2. July 21st

Time	Node Number							Relative Glider INS Position (m)			Distance from Center
	R10	R11	R12	R13	R14	R15	R21	Latitude	Longitude	Height	
06:58:40								-125.95	-543.41	101.00	566.88
06:58:46								-129.84	-544.00	101.00	568.32
06:58:48								-131.32	-544.90	101.00	569.53
06:58:53								-132.24	-545.70	101.00	570.51
06:59:00								-132.80	-546.61	101.00	571.50
06:59:04								-133.17	-547.41	101.00	572.36
07:03:45	805.5		1791.9	1559.8	754.6	452.5	2388.6	-93.34	-508.77	41.55	518.93
07:05:56	777.4	1345.5		1519.5				-92.26	-474.68	36.13	484.91
07:08:32	719.2	1330.3		1480.5	722.1	519.6	2299.9	-92.64	-417.39	71.84	433.54
07:12:24		1305.3	1636.8	1387.3	692.1	570.0		-94.80	-359.86	60.46	377.01
07:14:37		1281.1		1350.7		595.2	2173.3	-92.96	-328.38	39.43	343.55
07:16:20	571.8				679.2	634.8		-89.99	-303.33	34.42	318.26
07:18:47	531.1	1265.1		1277.7	673.5		2088.9	-89.95	-247.78	69.80	272.68
07:20:52		1254.3	1477.3	1223.5	677.2	707.2	2045.1	-90.80	-212.83	77.84	244.13
07:22:49	468.3	1259.5	1457.4	1201.5	666.4		2014.6	-91.17	-188.36	62.35	218.35
07:24:57	442.9	1248.6	1428.3	1164.3	792.9		1967.8	-91.24	-155.15	41.41	184.69
07:27:16	407.7	1248.3		1133.4	667.8	790.8	1942.2	-86.29	-120.34	37.71	152.81
07:29:05	379.2		1378.8	1086.6	673.2			-88.55	-78.79	64.14	134.77
07:31:03	353.2		1322.1	1036.0	695.7	883.2	1845.9	-87.43	-39.14	79.09	124.22
07:34:08	338.2	1256.2	1290.1		699.0	926.2	1797.0	-90.25	5.26	50.96	103.78
07:35:59	310.8	1270.2	1266.6	972.4				-88.91	31.01	34.66	100.34
07:37:41	302.8				712.6			-84.04	59.44	40.43	110.59
07:39:43	298.3	1276.0	1231.0	896.2			1691.8	-86.93	105.16	69.61	153.17
07:43:02	304.2	1295.1		843.4	759.0			-87.56	157.94	66.42	192.42
07:45:15	303.3	1300.0	1177.2	816.1	770.4		1598.8	-89.26	184.61	48.75	210.77
07:49:25	322.3	1332.4	1108.9	754.6	809.2		1532.2	-84.85	250.56	51.25	269.45
07:51:33	343.3	1340.4	1082.7	710.1	835.5		1511.4	-86.81	298.54	81.53	321.41
07:53:38	376.5		1058.5	668.7			1453.8	-87.70	328.06	69.06	346.53
07:55:34	392.1	1366.6	1037.7	640.2	879.1		1415.7	-88.88	351.67	52.81	366.55
07:58:52	424.6	1403.1	1018.9	588.6		1356.1		-84.26	396.72	35.28	407.10
08:00:52	463.3	1412.8	998.4	558.9	937.8		1342.8	-86.32	441.91	63.25	454.69
08:03:37	511.0		967.2	504.7			1261.8	-88.20	490.44	75.04	503.93
08:05:34	536.8	1460.5	960.1	488.8		1479.6	1248.6	-86.84	517.00	57.52	527.39
08:07:28	570.1	1473.6		457.3			1201.3	-73.42	550.41	70.80	559.78
08:09:31	582.9	1475.5	911.1	450.4	1072.6		1166.5	-31.21	584.89	99.05	594.04
08:10:35								-409.12	271.37	101.00	501.22
08:11:26	584.5	1494.4	912.3	464.2	1134.7	1581.6					
08:13:18	580.9		888.6	465.6		1576.6					
08:15:26	572.1		915.7			1566.6					
08:17:31	559.8			481.9							
08:19:18	548.7		943.9	492.0							
08:22:04	537.9		949.6	502.0	1101.4						
08:24:00	531.0		952.6		1092.6	1521.9					

08:25:48	526.3		958.8		1086.3						
08:29:16								-383.41	221.49	101.00	454.16
08:29:23								-382.85	221.49	101.00	453.69
08:29:27								-382.85	221.18	101.00	453.54
08:29:32								-382.85	220.98	101.00	453.44
08:29:37								-382.48	220.58	101.00	452.94
08:29:41								-382.11	220.08	101.00	452.38
08:33:16	494.7	1409.2	925.0	527.8				-354.62	236.19	62.00	430.57
08:35:50	508.2	1415.4		514.2		1482.7	1207.6	-329.12	265.17	37.30	424.30
08:38:05	519.4	1413.3		508.6	1083.0	1507.8	1189.5	-293.88	296.26	44.34	419.64
08:40:04	537.7	1410.6		509.2	1115.5	1520.4	1165.5	-263.40	334.83	73.32	432.28
08:42:00	570.3	1409.5	812.4	511.9	1153.8	1568.5		-240.54	361.22	76.73	440.71
08:43:56	580.3		802.5	506.5	1174.3	1582.2	1105.9	-219.84	380.13	61.62	443.43
08:45:55	592.2	1416.0		508.6	1199.5	1589.5	1079.7	-201.87	402.91	44.65	452.86
08:48:23		1425.0	759.4	510.0	1244.7		1058.7	-171.65	431.02	35.45	465.29
08:50:18	626.4	1417.2	735.3	514.6		1629.0	1043.1	-139.24	468.48	62.52	492.72
08:52:14	661.8	1427.8	703.0	527.1			1005.1	-108.88	501.44	80.76	519.44
08:54:53	691.3	1435.0	685.8	532.9			970.8	-79.64	527.10	69.23	537.56
08:56:55	700.0	1427.2	660.9	554.2	1350.1	1724.4	958.0	-16.30	528.23	96.12	537.15
08:58:14								-243.95	405.01	101.00	483.47
08:58:51	664.8	1417.5	641.7	592.6	1374.7						
09:00:47		1411.0	642.4	596.7			1044.7				
09:03:26	651.9				1367.5						
09:05:18	647.8		638.8	604.2	1367.8						
09:06:54								-243.58	404.70	101.00	483.03
09:07:12	648.1		637.9	605.2	1370.2			-239.99	403.42	101.00	480.15
09:07:56								-231.01	400.20	101.00	473.00
09:08:01								-230.08	400.00	101.00	472.38
09:08:06								-229.90	400.11	101.00	472.38
09:08:11								-230.08	400.31	101.00	472.64
09:08:17								-229.71	400.31	101.00	472.46
09:08:21								-229.53	400.21	101.00	472.28
09:08:26								-229.53	400.31	101.00	472.37
09:10:48	637.2	1357.8	633.9	608.1	1332.0	1639.0	1040.1	-201.58	401.28	75.37	455.35
09:12:45	634.3	1347.4	616.5	622.8			1018.9	-172.88	414.06	57.56	452.38
09:14:39	633.9	1336.8	729.4	643.9				-141.77	427.13	39.10	451.74
09:30:52	607.5	1193.8	497.2				1093.5	145.13	453.98	80.66	483.39
09:38:19			533.1	807.9			1159.0	206.80	352.64	41.70	410.92
09:40:24	373.6		668.1	836.2	1261.0	1394.8		234.20	311.77	71.90	396.51
09:43:28	315.6		731.8		1205.1		1396.6	262.44	270.87	67.83	383.20
09:48:48		1010.2		916.0	1149.0		1468.6	299.12	207.02	35.06	365.46
09:50:41	141.1	1000.6		948.0	1100.5			319.79	169.28	61.18	366.97
09:56:59	99.4				1032.4	1035.7	1675.5				
09:58:57	103.8	1068.6		1042.5	1043.5	1059.7					
10:00:51	103.0	1023.7			1041.4	1005.7					
10:03:24	143.4	1024.6		1026.4	1013.2						
10:05:13	104.5	1046.7		1029.6	1012.8						
10:07:42		1092.4		1057.3	1033.6	1013.8					

10:11:06	107.8	1057.3			1035.9	1001.7					
10:12:57	108.1	1046.4			1040.8	975.0					
10:15:35	107.5	1018.3		1080.7	1051.9		1711.6	182.28	47.96	101.00	213.84
10:16:10								12.76	-19.38	101.00	103.63
10:16:16								13.13	-19.08	101.00	103.62
10:16:21								13.50	-18.68	101.00	103.60
10:16:26								14.06	-18.37	101.00	103.62
10:16:31								14.24	-18.37	101.00	103.64
10:16:36								14.24	-18.07	101.00	103.59
10:18:56	100.0	977.8	1021.5	1050.7	1022.7	970.3	1689.1	36.99	-34.51	75.89	91.20
10:20:46	104.7	959.8	1022.8			938.4	1723.2	65.68	-47.75	56.46	98.90
10:25:14	140.4				1023.1	917.7		148.48	-94.46	50.80	183.16
10:28:12	256.6	895.2	1162.5	1235.1		789.7	1877.4	216.14	-127.10	79.85	263.15
10:30:49	296.5	875.4	1197.3				1924.8	253.01	-146.05	59.65	298.16
10:33:27	341.8		1230.1	1343.1		687.3		303.69	-167.02	31.71	348.03
10:35:20		858.0			1074.4	651.9		337.81	-190.22	45.17	390.30
10:37:21	442.3	847.9	1306.3		1095.3	613.5		395.98	-216.66	78.02	458.07
10:42:49	531.9	823.3	1395.0		1133.8	518.4	2182.0	487.55	-263.73	40.42	555.78
10:48:53		834.0	1500.9		1198.2	421.9	2298.9	622.65	-331.91	79.16	710.02
10:51:36		837.6	1532.4	1685.7		399.6	2335.8	610.37	-369.21	100.79	720.44
10:52:15								425.21	-411.94	101.00	600.58
10:56:27								442.22	-396.10	101.00	602.21
10:56:34								442.78	-395.90	101.00	602.48
10:56:38								443.15	-395.80	101.00	602.69
10:56:43								443.15	-395.19	101.00	602.29
10:56:47								443.33	-395.19	101.00	602.43
10:56:53								443.52	-395.19	101.00	602.56
11:00:16	763.3			1751.1	1297.0	404.1		482.08	-387.35	66.30	621.97
11:02:54	761.2		1538.7	1759.9		506.5		528.15	-371.49	38.31	646.85
11:05:03			1536.9	1768.8		443.4		576.93	-359.33	39.76	680.84
11:07:04	796.3	710.4	1529.5			469.5	2385.9	629.46	-337.26	65.53	717.12
11:09:40	808.2	683.8	1495.6	1780.0	1401.7	514.2	2359.5	587.13	-317.23	74.49	671.50
11:12:07	737.5	705.7	1478.5	1729.3	1347.6	487.3	2325.7	540.33	-305.73	51.69	622.98
11:14:17	690.0	734.7	1460.7	1681.0	1293.3	477.7	2307.6	499.20	-298.04	32.04	582.29
11:16:17			1454.5		1250.7	485.7	2273.5	450.51	-283.15	47.89	534.25
11:19:36	579.6	827.5	1423.9	1563.0		503.1	2203.2	359.86	-265.91	79.09	454.39
11:21:35	544.9		1416.3			501.3	2180.8	320.35	-259.44	62.14	416.88
11:23:41	523.6	895.2	1413.4	1484.4		510.1	2158.9	281.51	-251.72	45.04	380.31
11:25:47	518.7		1409.4				2147.8	245.79	-240.83	29.53	345.38
11:28:35	504.6		1414.5	1420.2	979.5		2131.6	164.17	-222.02	66.48	284.02
11:32:05	437.4			1331.4	882.1	607.5	2062.6	86.32	-207.62	67.41	234.73
11:37:34			1415.8		784.0		2016.7	-17.43	-184.14	37.96	188.82
11:39:32	418.6		1416.3	1204.5	727.2	735.0	2010.9	-74.89	-170.79	64.58	197.35
11:41:26	435.3		1433.7		678.4		1980.7	-127.54	-161.72	81.02	221.32
11:44:05	453.1		1427.7	1133.4	643.8		1949.5	-173.08	-152.05	60.81	238.27
11:46:12	459.7		1439.5		595.3		1932.1	-210.62	-143.21	42.75	258.25
11:50:39	499.8		1455.0	1024.0	528.7	949.5	1907.8	-319.04	-113.14	66.76	345.03
11:52:44	541.2			991.5	488.2			-371.99	-101.94	78.19	393.55

11:55:04	567.4		1484.1	971.1	455.8	1019.1	1868.1	-418.23	-92.92	56.89	432.19
11:57:05			1497.0		422.8	1065.7	1857.7	-455.73	-82.79	38.66	464.80
11:59:08	619.6	1581.1	1510.0	927.6	404.8		1850.2	-500.19	-70.71	38.82	506.65
12:01:24	667.9		1529.8	903.7	388.3	1137.1	1832.7	-566.80	-54.49	69.50	573.64
12:04:06	716.1		1551.9	865.3	372.4		1815.0	-631.83	-39.46	69.76	636.89
12:11:32	836.5		1617.9	829.2	361.8		1796.8	-800.77	-0.82	67.46	803.61
12:13:36	986.4		1663.9	808.8	386.2		1792.3	-864.35	12.97	99.45	870.15
12:14:43								-896.84	-137.23	101.00	912.88
12:20:46					433.3	1480.9					

3. July 22nd

	Node Number							Relative Glider INS Position (m)			Distance from Center
Time	**R10**	**R11**	**R12**	**R13**	**R14**	**R15**	**R21**	**Latitude**	**Longitude**	**Height**	
07:13:54								39.21	-670.54	101.00	679.24
07:13:59								38.47	-671.05	101.00	679.69
07:14:03								37.55	-671.65	101.00	680.24
07:14:08								36.62	-672.05	101.00	680.58
07:14:12								35.88	-672.25	101.00	680.74
07:14:20								35.14	-672.75	101.00	681.19
07:14:24								34.22	-673.15	101.00	681.54
07:16:03	993.6		1980.7		956.1	313.6	2622.6	40.55	-659.78	80.23	665.88
07:22:36			1863.7	1709.5	923.5	283.9		95.26	-572.66	46.92	582.42
07:24:49	835.9		1806.9	1678	914.5	300.4		114.09	-524.12	80.82	542.45
07:26:44	793			1629.6				109.06	-499.51	73.22	516.49
07:29:10	761.7			1605.3	889.8	346.2	2387.2	111.97	-467.65	52.29	483.70
07:31:11	719.5	1190.4	1706.8	1567.8	880.5	368.4		108.81	-439.66	33.90	454.19
07:34:27	655.9	1168.6	1628.7	1503.1	857.7	438.1	2278.2	114.04	-373.89	65.28	396.31
07:36:33	607.9	1153	1571.4	1460.5	848.4	487	2231.5	113.98	-335.33	78.68	362.81
07:38:28	570.7	1140.1	1541.1	1421.1	840.9	507.3	2190.3	110.34	-311.99	63.96	337.06
07:40:23	535.5		1520.4	1391.8	827.2	530.8		113.77	-288.81	49.02	314.25
07:42:36	502.5	1121.7		1361.1	825.6		2123.4	111.51	-261.24	31.56	285.79
07:46:20	429.7		1407.4	1286.5	812.5			113.47	-184.61	75.12	229.35
07:48:51	379.9	1112.4		1223.1	814			114.92	-145.80	68.92	198.03
07:50:47	358.2	1108	1340.1		813		1951.8	113.78	-142.51	66.68	194.17
07:52:53	313	1104.9	1332.1	1173.9	814.6	753.3	1923.9	111.86	-97.08	36.67	152.59
07:54:47	284.7		1275.6		828.7		1888.2	116.44	-66.64	40.23	140.07
07:56:50	249.4		1259.2	1097.8	819.6	828.3	1840.6	112.11	-21.55	68.43	133.10
07:58:42	222.7	1114.8	1222.5		839.1			113.71	12.18	79.00	138.99
08:00:46	226.8	1123	1176.7	1025.2	839.8	916.8	1758	110.86	36.57	62.79	132.55
08:03:11	179.4	1127.4					1731.9	113.18	67.78	41.42	138.28
08:05:10	162.9	1139.8	1129.6		861.6		1686	115.76	95.81	34.49	154.17
08:07:13	160.9	1151.1	1096.3	917.2	867		1644.9	115.51	140.71	62.96	192.63
08:09:10	175.5		1062.3	878.1		1072.6	1597	112.50	179.06	80.33	226.21
08:11:09	195.7		1032.1	845.7	904.5		1557.3	112.63	182.81	78.41	228.59
08:13:06	203.7	1190.1		822.4	915.3		1546.9	111.97	228.54	48.08	258.99
08:15:14	929.5			796.6	929.5		1498.8	113.54	257.26	29.40	282.74
08:18:29	274.3	1229.7	971.7	758.8	947.7		1471.3	113.52	324.93	69.67	351.17

08:20:10	329.7	1251.1						110.53	353.97	81.18	379.61
08:22:13	348.3	1276	913.6	760.3			1354.3	113.48	376.89	66.84	399.24
08:24:11	369.9		895.5	662.8			1343.1	110.08	401.14	49.85	418.94
08:26:14	395.1	1314.6	877	622.8			1309	111.08	428.02	31.23	443.30
08:28:12	431.2	1337.5		697.2			1266.3	115.18	465.30	48.62	481.80
08:30:10		1362.4		561.1	1090.8		1212.1	112.75	512.26	80.60	530.68
08:32:40						1503		-55.45	443.07	100.86	457.78
08:33:11								-331.25	279.58	101.00	445.07
08:34:37	543	1425.4		532		1555.6	1193.8				
08:36:59		1417.5		539.4			1211.7				
08:39:12	500.1	1410.7	855.9	549.7			1238.5	-332.14	234.31	101.00	418.83
08:39:15								-332.18	232.24	101.00	417.70
08:39:23								-331.99	231.84	101.00	417.33
08:39:24								-331.99	231.23	101.00	417.00
08:39:29								-331.99	230.33	101.00	416.50
08:39:35								-332.18	229.72	101.00	416.31
08:39:40								-331.99	229.02	101.00	415.77
08:41:08	483.9		865.9	560.8	1070.2			-316.85	240.84	81.32	406.21
08:43:31	483.6			560.4	1085.8	1462	1211.8	-282.52	263.87	53.38	390.25
08:45:32	488.7	1357.9		564.4	1119.1	1489.6		-253.56	281.62	33.64	380.44
08:48:56	518.8	1349.2	774.6	571.2				-178.60	330.82	66.54	381.79
08:51:11		1350.1	745.2	594.9	1197.3		1133.7	-135.37	361.30	76.10	393.26
08:53:07	540.1	1329.4	720.3					-107.93	382.05	57.89	401.20
08:55:21	559	1323.9		604.8		1565.7	1102.2	-73.74	403.44	36.79	411.77
08:57:20			680.8	609.1		1575.3	1089.7	-35.52	425.19	41.18	428.66
09:00:49	610.6	1320.4	620.7	642.7	1330.8		1052.1	37.91	477.85	80.57	486.07
09:03:34		1318.5	586.6	661.9		1631.4	1028.7	77.29	504.56	56.96	513.61
09:05:41	639.9	1311.4	560.5	671.8	1390.3	1646.4	1018.8	106.01	523.67	38.85	535.70
09:07:53	664.3	1311.1	549.4	691.5		1671.3	1005.1	162.31	543.90	62.53	571.03
09:09:56	661.6	1283.2	509.7	728.5	1436.2			228.31	542.43	91.16	595.54
09:11:35								-61.96	400.17	101.00	417.34
09:11:53	627.1	1266.9	501.7								
09:13:52	601.9		506.7	780.3		1623.9	1127.8				
09:16:00	575.4	1227.6	524.7			1590.3	1153.9				
09:20:14	514.5	1193.1	565.5				1213.2				
09:24:38	454.3		604.6			1471.8	1269.4				
09:26:53	423.6		629.5								
09:28:36	403		647.7				1321.5				
09:30:23	381.7		669			1400.2	1342.8				

THIS PAGE INTENTIONALLY LEFT BLANK

INITIAL DISTRIBUTION LIST

1. Defense Technical Information Center
   Ft. Belvoir, VA

2. Dudley Knox Library
   Naval Postgraduate School
   Monterey, CA

3. Allen Moshfegh
   Defense Advanced Research Projects Agency
   Arlington, VA

4. Tom Swean
   Office of Naval Research
   Arlington, VA

5. Tom Curtin
   Office of Naval Research
   Arlington, VA

6. Doug Ray
   Naval Undersea Warfare Center, Keyport
   Keyport, WA

7. Chris Mailey
   Space and Naval Warfare Systems Center, San Diego
   San Diego, CA

8. Paul Baxley
   Space and Naval Warfare Systems Center, San Diego
   San Diego, CA

9. Chris Fletcher
   Space and Naval Warfare Systems Center, San Diego
   San Diego, CA

10. Bob Creber
    Space and Naval Warfare Systems Center, San Diego
    San Diego, CA

11. Bill Marn
    Space and Naval Warfare Systems Center, San Diego
    San Diego, CA

12. Doug Horner
Naval Postgraduate School
Monterey, CA

13. Tony Healey
Naval Postgraduate School
Monterey, CA

14. Jeff Weekley
Naval Postgraduate School
Monterey, CA

15. Sean Kragelund
Naval Postgraduate School
Monterey, CA

16. Ben Wring
Naval Postgraduate School
Monterey, CA

17. ENS Matthew Hahn, USN
USS Paul Hamilton, DDG-60
Pearl Harbor, CA

18. LT Michael Reed, USN
Naval Postgraduate School
Monterey, CA

19. David Book
Naval Postgraduate School
Monterey, CA

20. CDR Melissa Smoot, USN
Naval Sea Systems Command, PMS NSW
Washington, D.C.

21. Mr. and Mrs. Albert Ouimet
Warnaco Technical Center
Westerly, RI

22. Ms. Kathryn Clark
Science Applications International Corporation
Annapolis, MD

23. LCDR Roger Ouimet, USN
Orion, Inc.
Fuquay-Varina, NC